Dtsch. Entomol. Z. 71 (2) 2024, 265–287 | DOI 10.3897/dez.71.125877

Integrative taxonomic revision of the grasshopper genera *Parapetasia* Bolívar, 1884, and *Loveridgacris* Rehn, 1954 (Orthoptera, Pyrgomorphidae), with description of a new species of *Loveridgacris*

Jeanne Agrippine Yetchom Fondjo[1,2], Martin Husemann[2], Armand Richard Nzoko Fiemapong[3], Alain Didier Missoup[1], Martin Kenne[1], Maurice Tindo[1], Oliver Hawlitschek[4], Tarekegn Fite Duressa[2,5], Sheng-Quan Xu[6], Wenhui Zhu[6], Claudia Hemp[7]

1 *Zoology Unit, Laboratory of Biology and Physiology of Animal Organisms, Graduate School in Fundamental and Applied Sciences, University of Douala, Douala, Cameroon*

2 *Staatliches Museum für Naturkunde Karlsruhe, Karlsruhe, Germany*

3 *University of Neuchâtel, Neuchâtel, Switzerland*

4 *Department of Evolutionary Biology and Environmental Studies, Universität Zürich, Zürich, Switzerland*

5 *School of Plant Sciences, College of Agriculture and Environmental Sciences, Haramaya University, Dire Dawa, Ethiopia*

6 *College of Life Sciences, Shaanxi Normal University, Xi'an, China*

7 *Senckenberg Biodiversity and Climate Research Center, Frankfurt, Germany*

https://zoobank.org/8108C5B0-40C9-40CA-A38B-8805F173900D

Corresponding author: Jeanne Agrippine Yetchom Fondjo (jayetchomfondjo@gmail.com)

Academic editor: Susanne Randolf ♦ **Received** 21 April 2024 ♦ **Accepted** 19 September 2024 ♦ **Published** 21 October 2024

Abstract

The taxonomic status of the Pyrgomorphid genera *Parapetasia* Bolívar, 1884, and *Loveridgacris* Rehn, 1954 is complex and challenging. Here, we use a combination of morphological, distributional, and genetic data to revise the two genera and provide new information on their diversity. We describe a new species, *Loveridgacris tectiferus* **sp. nov.**, from Tanzania and formally resurrect the status of *Parapetasia rammei* as a valid species within *Parapetasia*, resulting in two species in *Parapetasia* (*P. femorata* and *P. rammei*) and two in *Loveridgacris* (*L. impotens* and *L. tectiferus* **sp. nov.**). We also sequenced the COI and 16S genes of 10 Pyrgomorphidae species and provided the first phylogeny of the group. Our data show that all species are clearly distinct and represent molecular operational taxonomic units (mOTUs), with the exceptions of *L. impotens* and *L. tectiferus* **sp. nov.**, which are morphologically clearly distinct but for which the concatenated sequence alignments of the two individual gene datasets (COI and 16S) do not provide sufficient information. In addition, high interspecific distances were found between *Parapetasia* and *Loveridgacris*. Moreover, the complete mitogenomes of *L. impotens* and *L. tectiferus* **sp. nov.** were sequenced using next-generation sequencing technology. The total lengths of the assembled mitogenomes were 15,592 bp and 15,737 bp, representing 13 protein-coding genes, 22 transfer RNA genes, two ribosomal RNA genes and one D-loop region, respectively. To aid in identification, we present a key for the two genera, including a key to species. This study provides insights into the morphology, distribution, and phylogeny of Pyrgomorphidae in Africa.

Key Words

Afrotropical areas, cytochrome oxidase I, DNA barcoding, mitogenome, phylogeny

Introduction

The family Pyrgomorphidae, which has the type genus *Pyrgomorpha* Seville, 1838, is easily identifiable due to its unique phallic complex, which is relatively uniform within the family, as described by Dirsh in 1961. Members of this family are commonly referred to as gaudy grasshoppers and are renowned for their strikingly vivid coloration, which serves as a warning to predators. Pyrgomorphidae can sequester and accumulate plant secondary compounds, such as cardiac glycosides, from the toxic plants on which they feed. This accumulation leads to many species displaying aposematism, signaling their toxicity through conspicuous coloration. The Pyrgomorphidae family is the only member of the superfamily Pyrgomorphoidea and is closely related to the superfamily Acridoidea (Song et al. 2015). The presence of a groove in the fastigium and distinctive male phallic structures, including the cingulum that extends around the ventral side, medially directed endophallic apodemes, an ejaculatory sac that opens to the genital chamber, and undivided valves of the penis, differentiate the Pyrgomorphidae from other families, as noted by Kevan and Akbar (1964) and Dirsh (1961). Eades (2000) also described an ejaculatory sac opening to the genital chamber as a distinguishing characteristic.

The Pyrgomorphidae include 31 tribes, 149 genera, and 487 species (Mariño-Pérez and Song 2018) and are globally distributed. Most species of Pyrgomorphidae occur in tropical and subtropical countries of Africa, Asia, and Australia (Kevan and Akbar 1964; Mariño-Pérez and Song 2018). The tribe Dictyophorini, which includes only five genera with a small number of species each, namely, *Dictyophorus* Thunberg, 1815; *Maura* Stål, 1873; *Camoensia* Bolívar, 1882; *Parapetasia* Bolívar, 1884; and *Loveridgacris* Rehn, 1954, is distributed in Africa south of the Sahara (Kevan et al. 1974). The classification of the genera *Parapetasia* and *Loveridgacris*, as well as the species included in them, is complex. *Parapetasia* was first established by Bolívar in 1884 with *Parapetasia femorata* Bolívar, 1884, as the type by monotypy. *Loveridgacris* was first described by Karsch in 1888, with *Petasia impotens* Karsch, 1888, as the type that was later transferred to *Parapetasia* (Bolívar, 1904). Many researchers followed this classification and referred to *Petasia impotens* as *Parapetasia*. *Parapetasia rammei* Sjöstedt, 1923, the second species of *Parapetasia*, was described approximately 40 years later. Rehn (1953) conducted a partial revision of the genus *Parapetasia* in 1953 and separated the genus into two subgeneric entities based on the morphology of the pronotum and the size of the tegmina: *Parapetasia* (s.str) and *Loveridgea* (designated as a new subgenus). Rehn also distinguished two species within the subgenus *Parapetasia* (*Parapetasia*) based on female morphological features: the type species *Parapetasia femorata* and the newly described *Parapetasia calabarica* Rehn, 1953. In the subgenus *Loveridgea*, Rehn included two species, *P.* (*L.*) *impotens* and *P.* (*L.*) *ulugurensis*. Additionally, Rehn (1953) placed *P. rammei* Sjöstedt, 1923, in the subgenus *Parapetasia* (*Loveridgea*). Shortly thereafter, Rehn (1954) elevated the subgenus *Parapetasia* (*Loveridgea*) Rehn to *Loveridgacris* Rehn. Dirsh (1956), Johnston (1956), and Kevan (1962) maintained *P. rammei* in the subgenus *Loveridgacris* until Akbar and Kevan (1964) later raised the subgenus *Parapetasia* (*Loveridgacris*) to the generic status of *Loveridgacris* on the basis of phallic structures, with *L. impotens* and *L. ulugurensis* as the two species of this genus. Dirsh (1965), in his work on the genus *Parapetasia*, included five species distributed in Central, East, and West African forests, based on Rehn's descriptions: *Parapetasia femorata*, which was recorded in the lowlands of West African forest areas of the less elevated parts of Cameroon (Rehn 1953); *Parapetasia calabarica*, known only from southern Nigeria (Rehn 1953); *Parapetasia impotens* from Tanzania and southeastern Kenya; *Parapetasia ulugurensis* Rehn, 1953 from the Uluguru Mountains of Tanzania; and *P. rammei*, which was restricted to the more elevated areas of Cameroon. Shortly thereafter, Kevan et al. (1974) identified *L. ulugurensis* as a synonym of *L. impotens* and regarded *P. calabarica* and *P. rammei* as "almost undoubtedly mere forms of *P. femorata*." Later, Kevan (1977) effectively designated *P. calabarica* and *P. rammei* as true synonyms of *P. femorata*, with *P. calabarica* being the micropterous form and *P. rammei* being the brachypterous form. Mestre and Chiffaud (2009), based on Kevan's (1977) analysis, concluded that the genus *Parapetasia* is a monotypic Afrotropical genus.

The taxonomic status of species belonging to the genera *Parapetasia* and *Loveridgacris* remains challenging despite Kevan's (1977) attempt to synonymize some of the species. Some researchers, including Hochkirch (1998) and Seino and Njoya (2018), still consider certain species, such as *L. impotens*, *L. ulugurensis*, *P. femorata*, and *P. rammei*, to be distinct. Additionally, *P. rammei* shares many similarities with *L. impotens* in terms of morphology, coloration, and ecological preference, making it difficult to clearly differentiate between the two genera. To resolve this taxonomic confusion, molecular data may be useful. While some studies have generated DNA sequence data for *P. femorata*, none have focused on all species of these genera. Thus, we have conducted a comprehensive revision of the genera *Parapetasia* and *Loveridgacris* using an integrative approach that combines morphological studies, particularly of the phallic complex, with molecular analysis. Our study includes the description of a new *Loveridgacris* species and proposes a key to distinguishing valid species in both genera.

Materials and methods

Materials

Field collections and observations were made between 2020 and 2022 at five localities in three regions of Cameroon: Bekob and Iboti (Ebo forest in the littoral region), Manengouba Mountain (littoral region), Fotouni in the western highlands of Cameroon, and Somalomo in the Dja

Biosphere Reserve (eastern region). Furthermore, additional field trips were made at several locations in Tanzania. Individuals were collected by sight and hand using a sweep net. The collected specimens were deposited in the collections of the Karlsruhe Natural History Museum (SMNK) and the private collection of Claudia Hemp (CCH). In addition, some historical specimens belonging to the following collections have also been examined: the Hamburg Zoological Museum, Germany (ZMH), and the Museum für Naturkunde Berlin, Germany (MfN). Paratypes of *P. rammei* deposited at MfN Berlin and erroneously labeled as type (male) and allotype (female) were also examined.

Depositories

MfN: Museum für Naturkunde, Leibniz-Institut für Evolutions- und Biodiversitätsforschung, Berlin, Germany; **SMNK:** Staatliches Museum für Naturkunde Karlsruhe, Karlsruhe, Germany; **ZMH:** Zoologisches Museum Hamburg, Leibniz-Institut für Analyse des Biodiversitätwandels, Hamburg, Germany; **CCH:** Collection of Claudia Hemp.

Morphological analysis

Observations of external and internal morphological features were made with a Leica M165 C binocular microscope. Photographs of whole specimens were made with a high-resolution DUN Inc. stacking system (DUN Inc., California, USA).

Measurements were obtained using a digital caliper (at a scale of 0.01 mm). All measurements are given in millimeters (mm). For all measurements, males and females were measured separately. For each species, the following characters were examined: **HeadL:** length of head; **HeadW:** width of head; **AntenL:** length of antenna; **I.O.D.:** interocular distance; **FastigL:** length of fastigium of vertex; **PronotL:** pronotum length; **PronotW:** pronotum width; **TegL:** length of tegmina; **TL:** hind tibia length; **FL:** hind femur length; **fW:** hind femur width; and **BodyL:** body length, measured from the tip of the frons to the hindmost tip of the abdomen. The measurements of the specimens correspond to the average value of the different body parts plus the standard deviation (SD) of all newly collected samples, as well as all historical samples held by the ZMH and MfN (Germany).

Dissections and preparations of male and female genitalia followed the standard methods of Kevan et al. (1969) and Martinelli et al. (2017). The extracted internal genitalia were placed in a 1.5 mL microcentrifuge tube containing a solution of 5 µL proteinase K (20 mg/mL) and 25 µL buffer (pH 8.0, 10 mM Tris-Cl, 25 mM EDTA, 100 mM NaCl, 0.5% SDS) and were kept overnight in an incubator at 55 °C. The genitalia were gently separated from the digestion solution and then kept at 95 °C for 10 minutes to inactivate the enzyme. Preparations were then washed with double-distilled water (ddH_2O). Photographs of male and female genitalia were obtained with a Keyence VHX-7000 digital microscope (Clustermarket London, United Kingdom). The terminology for male genitalia and female spermatheca followed Dirsh (1956, 1957, 1970), Kevan et al. (1974), and Rowell (2013).

Distribution of species

Distributional data were obtained from geographical coordinates recorded during field observations, from locality records taken from specimen labels in different collections of museums, and from records available in the literature. A distribution map of the species was made using QGIS 3.28.3 "Firenze" (2023).

DNA extraction, PCR amplification, sequencing, and data depository

DNA was extracted from the femoral muscle tissue of 24 specimens stored in 96% ethanol. The species considered in this study are large; hence, only fragments of femoral muscles were used for DNA extraction at the Museum der Natur Hamburg. A high-salt extraction method was used (Paxton et al. 1996). The primer pair LCO and HCO (Folmer et al. 1994) was used for amplification of the COI gene, while the primer pair 16S-F and 16S-R (Palumbi et al. 1991) was used to amplify the 16S markers. The thermocycling conditions consisted of an initial denaturation at 94 °C (3 min), 35 cycles at 94 °C (denaturation, 30 s), 50 °C (annealing, 45 s), 72 °C (extension, 1 min), and a final extension at 72 °C (10 min). Samples were run on a 1% agarose gel stained with GelRed (Biotium, Remont, CA, USA) to test for amplification. Successfully amplified samples were purified with an ExoSap Enyzme cocktail (VWR, Pennsylvania, USA). The purified PCR products were then sequenced in both directions by Macrogen Europe (Amsterdam, Netherlands).

Phylogenetic analyses

Sequences were aligned and checked in GENEIOUS PRO (Kearse et al. 2012) using the MUSCLE algorithm (Edgar 2004). The aligned sequences included each one sequence of *Parapetasia femorata* (MT011522) and *Zonocerus elegans* (MT011544), which were downloaded from GenBank. We checked for pseudogenes (Numts) by translating sequences into amino acids using the invertebrate mitochondrial code and checking for frame shifts. Furthermore, the National Center for Biotechnology Information (NCBI) Blast and BOLD databases were used to check for species identity (a few related taxa are available in the databases). We used MRBAYES 3.2 (Ronquist et al. 2012) to reconstruct the phylogeny. For this, we used the reversible jump model. *Zonocerus elegans* was defined

as the outgroup. Analyses were run for 1 million generations, sampling every 100 generations for a total of 10 000 trees. The first 25% of the samples were discarded as burn-in. The average split frequencies were less than 0.01, indicating convergence of the analyses. The final tree was visualized with FIGTREE v.1.4.2 (Rambaut 2010). The net evolutionary divergence between groups of sequences was estimated using MEGA11 (Tamura et al. 2021).

Complete mitochondrial genome assembly, annotation, and analysis

For *L. impotens* and *L. tectiferus*, for which the phylogeny was not resolved when using only COI, the complete mitochondrial genome was sequenced by Novogene, China. Thereafter, the sequences were checked and assembled using MitoZ (Meng et al. 2019). All mitochondrial genes were further adjusted and corrected using GENEIOUS 10.1.3 (Kearse et al. 2012) with the reference mitogenome of *Oxya sinensis* (Thunberg, 1815). The base composition, codon distribution, and length of the protein-coding genes were calculated in Geneious Prime 2023.1.2 (Kearse et al. 2012). Nucleotide compositional differences (composition skew) were measured using the formula (A − T)/(A + T) for AT skew and (G − C)/(G + C) for GC skew (Perna & Kocher, 1995). The genetic distances for different PCGs among the two *Loveridgacris* species were estimated using MEGA 11 (Tamura et al. 2021).

Results

Taxonomy

Key to *Parapetasia* Bolívar and *Loveridgacris* Rehn

The genus *Parapetasia* can be easily distinguished from the genus *Loveridgacris* by several characters:

1 (2) Fastigium of vertex triangular; eyes small, hemispherical, prominent; pronotal disc sellate; posterior part of metazona raised, swollen, with median margin slightly or strongly emarginate (Fig. 2A, B, G, H); hind femora upper-median margin distinctly raised; elytra shortened, or, if brachypterous, slightly reticulated; male subgenital plate with slightly incised and parallel margins (Fig. 2E); epiphallic bridge narrow; appendices subparallel; ectophallus short; ventral process of cingulum broadly triangular (Fig. 6A, B, D, E, G, H, J, K) ..... *Parapetasia* Bolívar, 1884 (West and Central Africa)

2 (1) Fastigium of vertex rounded; eyes of moderate size, oval, not prominent; pronotal disc not sellate; posterior part of metazona not notably raised nor swollen, its median margin not emarginate (Fig. 2C, F, I); hind femora upper-median margin flat, not raised; elytra brachypterous, strongly reticulated; male subgenital plate with fused margins (Fig. 5A, B); epiphallic bridge wide or broad; appendices divergent; ectophallus elongate; ventral process of cingulum subtriangular (Fig. 6C, F, I, L)..... *Loveridgacris* Rehn, 1954 (East Africa)

Genus Parapetasia Bolívar, 1884

Parapetasia Bolívar, 1884 (type species: *Parapetasia femorata* Bolívar, 1884b, by monotypy).
Parapetasia (*Parapetasia*) Rehn, 1953
Parapetasia (*Loveridgea*) Rehn, 1953
Parapetasia (*Loveridgacris*) Rehn, 1954

Diagnosis of the genus *Parapetasia* Bolívar. Fastigium of vertex triangular; tegmina vestigial, or if brachypterous, strongly reticulated; the eyes small, hemispherical, and prominent; posterior part of metazona raised, swollen, with median margin slightly or strongly emarginate; hind femora upper-median margin distinctly raised; male subgenital plate with slightly incised and parallel margins; epiphallic bridge narrow; appendices subparallel; ectophallus short; ventral process of cingulum broadly triangular.

Differential diagnoses for species of *Parapetasia*. *Parapetasia femorata* can be easily distinguished from *Parapetasia rammei* by the following characters: tegmina dark brown, strongly reduced, vestigial, (yellow–brown with brown veins, shortened or brachypterous, semilobed in *P. rammei*); first and/or second abdominal segments with a lateral black band behind the insertion points of the femora (absent in *P. rammei*); anterior projections of epiphallus large (small in *P. rammei*); lateral plates subparallel (oblique or divergent in *P. rammei*); lophi large, strongly curved (very small, slightly curved in *P. rammei*); suprazygomal plate widely rounded (U-shapedin *P. rammei*); apodemal lobes only slightly produced ventrally (strongly produced ventrally in *P. rammei*); basal emargination of cingulum shallow (very deep in *P. rammei*); endophallic apodemes short (strongly elongate or slender in *P. rammei*).

Parapetasia femorata Bolívar, 1884

Figs 1A, B, 2A, D, G, 6A, D, G, J, 7A, D, G

Holotype. Gabon • ♀; 6687; Natural History Museum Vienna, Austria.

Synonyms. *Parapetasia* (*Parapetasia*) *calabarica* Rehn, 1953: 121, 122–124, pl. 2: f. 17, pl. 3: f. 26. Kevan et al. (1974): 229; Kevan (1977): 318 (new synonym).

Figure 1. Habitus images of *Parapetasia* and *Loveridgacris* species. **A.** *P. femorata* nymph; **B.** *P. rammei* nymph; **C.** *P. femorata* adult; **D.** *P. rammei* adult; **E.** *L. impotens* nymph; **F.** *L. impotens* adult (the black arrow points at the yellowish foamy secretion on the abdominal segment).

Parapetasia rammei Sjöstedt, 1923, p. 10–11, pl. 1: f. 1, 2. Kevan et al. (1974): 229; Kevan (1977): 318 (new synonym).

Material examined. Cameroon • 1 male, 1 female; Iboti in the Ebo Forest; 4.450°N, 10.450°E; 736 m; 07 Jan. 2022; J.A. Yetchom Fondjo leg. and A.R. Nzoko leg.; SMNK; CMJ244. • 1 female; Iboti in the Ebo Forest; 4.450°N, 10.450°E; 736 m; 07 Jan. 2022; J.A. Yetchom Fondjo leg.; SMNK; CMJ245. • 1 female; Somalomo in the Dja Biosphere Reserve; 3.371°N, 12.733°E; 06 Jun. 2022; A.R. Nzoko leg.; SMNK; CMJ1439. • 1 male; Bekob in the Ebo Forest; 4.350°N, 10.420°E; 936 m; 20 Mar. 2021; J.A. Yetchom Fondjo leg.; SMNK; CMJ598. • 6 females; Mukondje Farm, Mundame-Mungo Fluss; 25 Nov. 1904; R. Rohde leg.; ZMH. • 1 male, 4 females and 1 nymph; Esosung, Bakossi-Gebirge; 10 Sep. 1909; C. Räthke leg.; ZMH. • 3 males, 4 females, 4 nymphs; Esosung, Bakossi-Gebirge; 01 Nov. 1912; R. Rohde leg.; ZMH. • 1 male; Esosung, Bakossi-Gebirge; 1913; ZMH. • 2 females; Esosung, Bakossi-Gebirge; 1930; O. Kröber leg.; ZMH. • 3 males; Buea, south-West; 1891; S. Preuss leg.; MfN. • 1 male, 3 females; South; 1891; S. Preuss leg.; MfN. • 1 male, 1 female; Station Jaunde [Yaoundé], Centre; Mar. 1997; V. Carnap S.G. leg.; MfN. • 1 male, 1 female; Dibongo of Sanaga, Littoral; Ld. Kam leg.; MfN. • 1 male, 1 female; Lolodorf, South; L. Conradt S. leg.; MfN. • 1 female; Victoria [Limbe], south-West; S. Preuss leg.; MfN. • 1 female; Barombi station, south-West; Preuss S. leg.; MfN. • 1 male; Duala [Douala], Littoral; Dr Schäfer leg.; MfN. • 1 female; Nlobe-Ndunge; 500–700 m from Edea-Douala, Littoral; Dr Schäfer leg.; MfN. • 1 female; Longi; Jun. 1904; MfN. • 1 nymph; Japoma, Littoral; Dr Schäfer leg.; MfN. • 1 nymph; Victoria [Limbé], south-West; Jan. 1898–1899; MfN. • 2 females; north

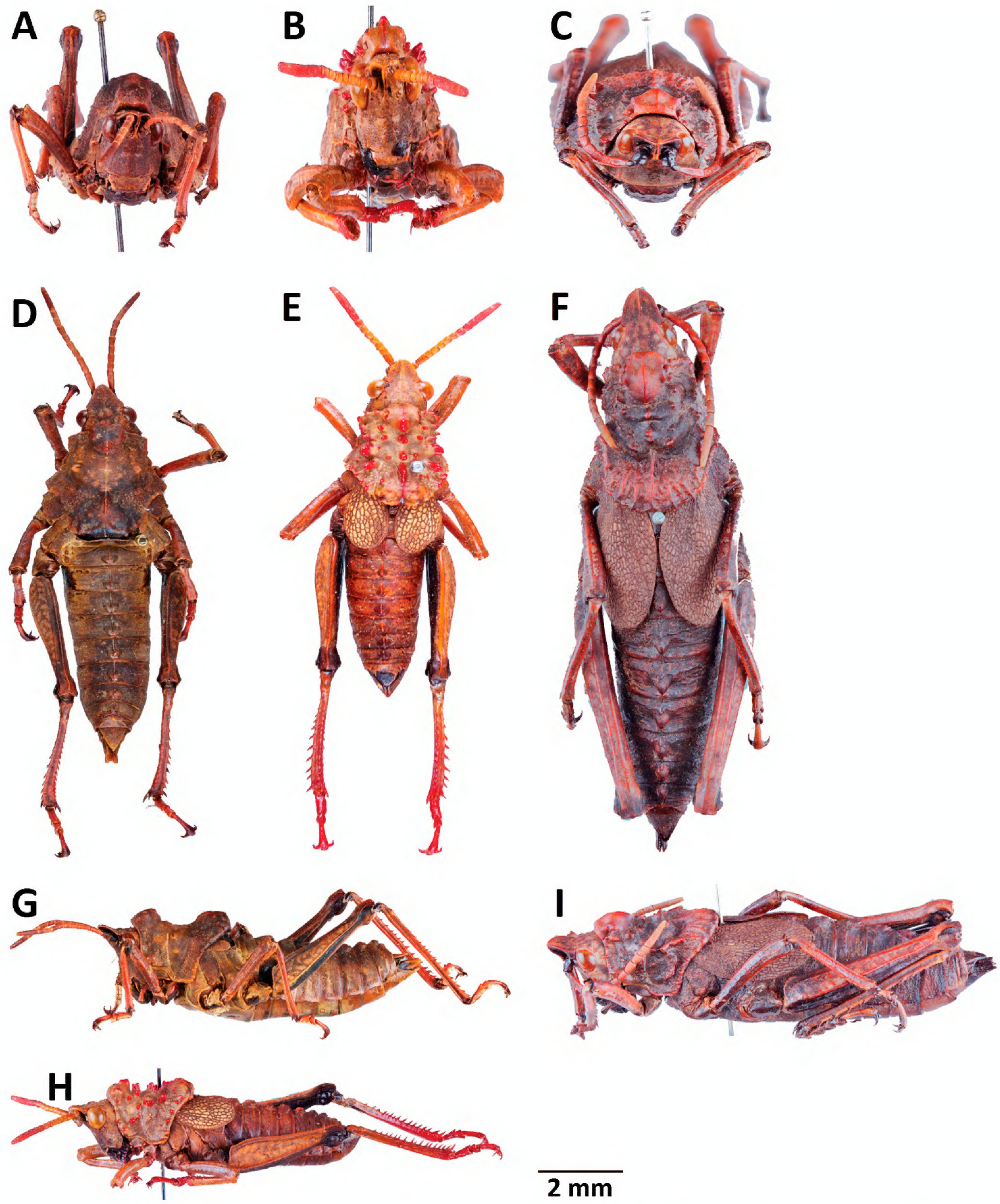

Figure 2. Frontal, dorsal and lateral views. **A–C.** Frontal view; **A.** *P. femorata*; **B.** *P. rammei*; **C.** *L. impotens*; **D–F.** Dorsal view; **D.** *P. femorata*; **E.** *P. rammei*; **F.** *L. impotens*; **G–I.** Lateral view; **G.** *P. femorata*; **H.** *P. rammei*; **I.** *L. impotens*.

Mundame, Elephantensee; 21 Jan.–15 Feb. 1996; S. Conradt leg.; MfN. • 1 female; Buea, south-West; MfN. • 1 female; Mundame; 1896; MfN. • 2 males; Bissika, Span. Guinea; Dr Escherich leg.; MfN.

Redescription. Male. ***Body*****:** robust, depressed, with very finely or moderately rugose and tuberculated integument. ***Head*** (Figs 1A, 2A, D, G): acutely conical; fastigium of vertex slightly curved upwards, flat, slightly concave in basal part, distinctly triangular, narrowing toward apex (Fig. 2D); frontal carina hardly visible; antennae thick, shorter, or only slightly longer than head and pronotum together, with short transverse or subtransverse segments, the last apical segment being distinctly longer than others. ***Thorax*** (Fig. 2D, G): pronotum with large inflation in front of first sulcus, strongly tuberculated in anterior part of prozona and posterior part of metazona, with the posterior part of the prozona and anterior part of the metazona being very finely tuberculated; median carinae inconspicuous and interrupted, lateral carinae absent; inferior margins of lateral lobes of pronotum straight; prozona shorter than metazona; posterior margin of metazona strongly emarginate; prosternal process very short, subacute or obtuse-angular; mesosternal interspace wider than long. ***Legs*** (Fig. 2D, G): hind femur slender, its external area not expanded, its upper-median margin distinctly

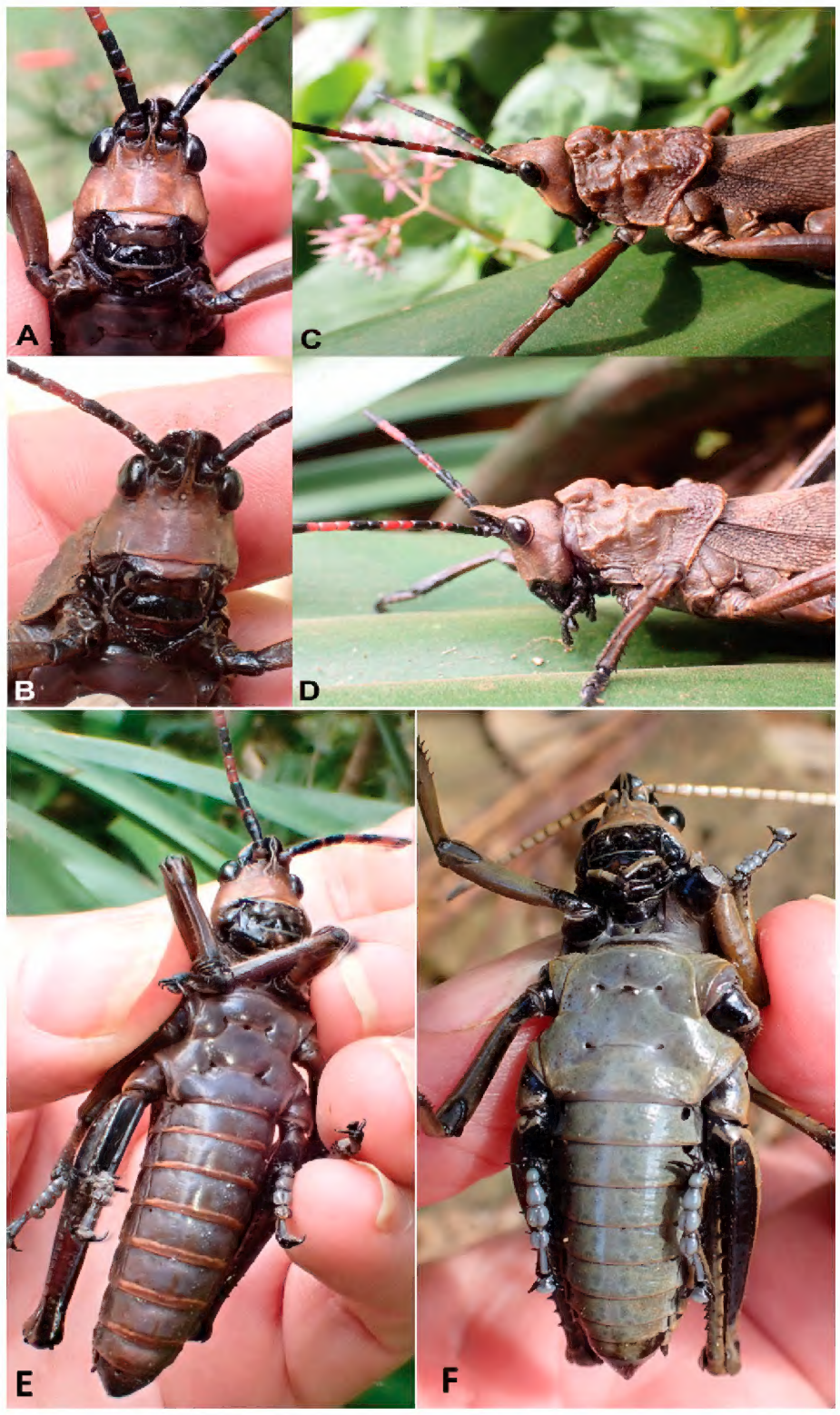

Figure 3. A–E. *L. tectiferus* sp. nov. **A.** Male in frontal view; **B.** Female in frontal view; **C.** Male head and pronotum; **D.** Female head and pronotum; **E.** Male in ventral view; **F.** Male of *L. impotens* in ventral view.

raised; obliquely expanded area at the base of hind femur strongly pronounced; external apical spine of hind tibiae present; hind tarsal segments not elongate. ***Elytra*** (Fig. 2G): strongly reduced, micropterous, not reaching point of insertion of metathoracic legs, with rounded posterior margins. ***Abdomen*** (Fig. 2D): often annulated; abdominal tergites each with a trigonal medio-dorsal tubercle; male supra-anal plate subtriangular; male subgenital plate compressed toward apex above, margins slightly incised, parallel; male cerci conical (Fig. 7A). ***Epiphallus*** (Fig. 6A): bridge narrow, its anterior margin emarginate; anterior projections large, fairly prominent, not broadly rounded; appendices broad, subparallel, with apical lobes having smaller and broader processes, attached marginally to the basal part of the lateral plates; lateral plates subparallel, almost straight, directed posteriorly, with external margins not expanded; lophi large, strongly curved upward, anteriorly directed with acute apex. ***Ectophallus*** (Fig. 6D, G, J): central membrane fairly narrow, rather triangular or subtriangular, marked at its lateral margins by furrows; zygoma broadly transverse, not extending halfway along the cingulum; suprazygomal plate widely rounded, moderately wide, highly shorter than the zygoma; apodemal lobes only slightly produced ventrally, the apices fairly wide apart; valves of cingulum small, narrow, and divergent in dorsal view; rami of cingulum rather broad in dorsal view, extending into sheath; dorsal cleft of cingulum rather narrow, ventral cleft small; suprarami well developed; basal emargination of cingulum shallow; sheats rather well developed; ventral process of cingulum short, not reaching the apex of endophallic apodemes nor the basal thickening of cingulum in ventral view. ***Endophallus*** (Fig. 6D, G, J): endophallic apodemes broad or stout, rather short, not reaching the basal emargination of cingulum in ventral; aedeagal valves narrow, slender with button-like apices; aedeagal sclerites stout and shorter, ventrally directed; spermatophore sac small, ovoid, not extending beyond the lateral limits of endophallic apodemes; gonopore at the middle.

Female. As in male, but larger. ***Abdomen*** (Fig. 7D): subgenital plate in female without carina or keel, its posterior margin rounded and smooth; egg guide prominent, conical, and slightly elongated; ovipositor valves large, not sinuate. ***Genitalia*** (Fig. 7G): spermatheca thick, lacking an apical pocket, with a laminated appearance in the apical part; median longitudinal groove of genital chamber reduced; spermatheca duct short, with an elongate, terminally thickened region; secondary diverticulum of spermathecal appendage of varying shape.

Color. Predominantly brownish, sometimes with orange or red markings; eyes entirely black in adults; antennal scape black; head brownish, margin of vertex, antennae light brown or dark brown in some parts in adults; sternum light brown and black in some parts; dorsal part of mesothorax with a broad black band bordered laterally by the elytra; elytra dark brown; first and/or second abdominal segments with a lateral black band behind the insertion points of the femora; lower external, lower internal, and medial internal hind femoral areas blackish; fore and middle femora, outer-medial, upper-external and upper-internal areas of hind femora dark-brown; hind tibiae light brown; tarsi light brown; cerci black.

Nymph (Fig. 1A). Eyes dark-red; antennae predominantly black with yellow apex; hind knee predominantly yellow with black median mark.

Measurements. Male. Body length 37.80–40.45 mm; Female. Body length 45.98–62.69 mm. Adult *P. femorata* individuals exhibit very large size variations in both sexes. Additional information on the measurements is given in Table 1.

Geographical distribution (Fig. 8). *Parapetasia femorata* has been recorded from Gabon, Cameroon, Nigeria, and Equatorial Guinea. In Cameroon, *P. femorata* was discovered in two localities within the proposed Ebo Forest, namely, Bekob and Iboti, as well as in Somalomo, a location within the Dja Biosphere Reserve, and Ngoutadjap and Zamakoe.

Table 1. Measurements in millimeters (mm) of the examined *Parapetasia* and *Loveridgacris* species; n: number of individuals; FastigL: length of fastigium of vertex; PronotL: pronotum length; PronotW: pronotum width; TegL: length of wings; TL: hind tibia length; FL: hind femur length; Fw: hind femur width; and BodyL: body length, measured from the tip of the frons to the hindmost tip of the abdomen.

Species	*Parapetasia femorata* Bolívar, 1884				*Parapetasia rammei* Sjöstedt, 1923			
Parameters	Male		Female		Male		Female	
	(Mean ± SD)	(Range)	(Mean ± SD)	(Range)	(Mean ± SD)	(Range)	(Mean ± SD)	(Range)
HeadL	6.06 ± 0.43 (n = 5)	5.69–6.54	7.30 ± 0.98 (n = 15)	5.50–9.11	5.18 ± 0.32 (n = 2)	4.95–5.40	6.23 ± 0.57 (n = 7)	5.32–6.81
HeadW	5.03 ± 0.42 (n = 5)	4.53–5.58	6.22 ± 0.31 (n = 15)	5.53–6.61	4.51 ± 0.05 (n = 2)	4.47–4.54	5.33 ± 0.31 (n = 7)	5.09–5.96
AntenL	14.99 ± 1.33 (n = 5)	13.13–16.49	16.68 ± 1.56 (n = 15)	12.84–18.61	11.65 ± 0.53 (n = 2)	11.27–12.02	13.85 ± 0.61 (n = 7)	13.00–14.52
I.O.D.	2.69 ± 0.14 (n = 5)	2.51–2.82	3.34 ± 0.17 (n = 15)	3.06–3.63	2.77 ± 0.02 (n = 2)	7.75–2.78	3.30 ± 0.17 (n = 7)	3.15–3.66
FastigL	2.24 ± 0.27 (n = 5)	1.83–2.54	3.02 ± 0.39 (n = 15)	2.46–3.80	1.88 ± 0.01 (n = 2)	1.87–1.89	2.78 ± 0.30 (n = 7)	2.41–3.04
PronotL	10.94 ± 0.73 (n = 5)	10.08–11.64	13.84 ± 0.92 (n = 15)	12.41–15.37	10.37 ± 0.11 (n = 2)	10.29–10.44	13.50 ± 0.77 (n = 7)	12.63–14.64
PronotW	9.59 ± 0.58 (n = 5)	8.73–10.25	12.81 ± 0.79 (n = 15)	11.41–14.22	0.81 ± 0.59 (n = 2)	8.39–9.23	11.28 ± 0.61 (n = 7)	10.26–12.11
TegL	2.71 ± 0.82 (n = 5)	1.96–3.86	4.14 ± 0.89 (n = 15)	2.53–5.48	10.29 ± 0.76 (n = 2)	9.75–10.83	15.03 ± 1.11 (n = 7)	13.15–16.60
TL	16.01 ± 0.87 (n = 5)	15.15–17.27	19.69 ± 1.26 (n = 15)	17.10–21.26	13.07 ± 0.83 (n = 2)	12.48–13.65	17.23 ± 0.81 (n = 7)	15.86–18.04
FL	17.62 ± 1.04 (n = 5)	16.47–19.12	21.89 ± 1.31 (n = 15)	19.15–23.47	15.10 ± 0.21 (n = 2)	14.95–15.25	19.64 ± 0.58 (n = 7)	18.83–20.31
FW	3.65 ± 0.07 (n = 5)	3.55–3.71	4.47 ± 0.37 (n = 15)	3.77–5.08	3.55 ± 0.27 (n = 2)	3.36–3.74	4.17 ± 0.21 (n = 7)	3.87–4.49
BodyL	38.60 ± 1.06 (n = 5)	37.80–40.45	54.00 ± 5.06 (n = 15)	45.98–62.69	31.10 ± 1.80 (n = 2)	32.83–35.37	45.75 ± 2.40 (n = 7)	43.22–49.73

Species	*Loveridgacris impotens* (Karsch, 1888)				*Loveridgacris tectiferus* Hemp sp. nov.			
Parameters	Male		Female		Male		Female	
	(Mean ± SD)	(Range)	(Mean ± SD)	(Range)	(Mean ± SD)	(Range)	(Mean ± SD)	(Range)
HeadL	8.32 ± 0.42 (n = 2)	8.02–8.62	8.63 ± 0.48 (n = 4)	8.19–9.12	7.41 (n = 1)	NA	6.87 ± 0.60 (n = 2)	6.44–7.29
HeadW	7.11 ± 1.09 (n = 2)	6.34–7.88	7.10 ± 0.47 (n = 4)	6.40–7.41	8.95 (n = 1)	NA	9.18 ± 0.53 (n = 2)	9.55–8.81
AntenL	19.41 ± 3.13 (n = 2)	17.19–21.62	20.42 ± 1.21 (n = 4)	19.21–22.10	21.30 (n = 1)	NA	19 ± 00 (n = 2)	19.00–19.00
I.O.D.	3.55 ± 0.17 (n = 2)	3.43–3.67	4.17 ± 0.22 (n = 4)	3.99–4.49	4.10 (n = 1)	NA	4.20 ± 0.14 (n = 2)	4.10–4.30
FastigL	3.67 ± 0.34 (n = 2)	3.43–3.91	3.89 ± 0.30 (n = 4)	3.46–4.15	3.50 (n = 1)	NA	3.05 ± 0.07 (n = 2)	3.00–3.10
PronotL	16.05 ± 1.44 (n = 2)	15.03–17.06	16.41 ± 1.75 (n = 4)	14.54–18.70	13.6 (n = 1)	NA	21.60 ± 0.14 (n = 2)	21.50–21.70
PronotW	13.39 ± 1.22 (n = 2)	12.52–14.25	13.53 ± 1.34 (n = 4)	11.89–15.11	9.30 (n = 1)	NA	9.50 ± 00 (n = 2)	9.50–9.50
TegL	14.96 ± 2.02 (n = 2)	13.53–16.38	17.88 ± 1.54 (n = 4)	16.59–19.80	29.00 (n = 1)	NA	27.70 ± 0.71 (n = 2)	27.20–28.20
TL	21.62 ± 1.11 (n = 2)	20.83–22.40	24.20 ± 1.12 (n = 4)	22.99–25.69	20.67 (n = 1)	NA	23.19 ± 00 (n = 2)	23.19–23.19
FL	24.12 ± 0.69 (n = 2)	23.63–24.60	27.29 ± 0.75 (n = 4)	26.19–27.85	25.00 (n = 1)	NA	24.25 ± 0.49 (n = 2)	23.90–24.60
FW	4.25 ± 0.22 (n = 2)	4.09–4.40	4.82 ± 0.34 (n = 4)	4.40–5.11	3.44 (n = 1)	NA	4.65 ± 0.21 (n = 2)	4.80–4.50
BodyL	55.54 ± 6.58 (n = 2)	50.88–60.19	58.66 ± 6.77 (n = 4)	48.72–63.69	51.20 (n = 1)	NA	50.65 ± 4.17 (n = 2)	47.70–53.60

The measurements represent the average value of the different body parts plus the standard deviation (SD). The range reffers to the minimum and maximum values.

Ecology. *Parapetasia femorata* is distributed throughout the lowlands of West and Central Africa and is exclusively found in forest habitats with a closed canopy and close proximity to marshy areas, where litter is abundant. Within forest habitats, the species is geophilous. *Parapetasia femorata* is present throughout the year in Cameroon, with the highest abundance observed during the dry season from November to January. This species is known to produce foamy secretions on tergites 3 and 4.

Parapetasia rammei Sjöstedt, 1923

Figs 1C, D, 2B, E, H, 6B, E, H, K, 7B, E, H

Holotype. Cameroon • ♀; Bare-Dschang, [Stockholm]

Paratypes. Cameroon • 1 ♂, Bamenda; Adametz S.G. leg.; MfN URL: http://cool.mfn-berlin.de/u/bb659e [MfN]. • 1 ♀; Bangwe; 1000 m; Mitte V-Mitte VI. 99 [mid-May.–mid-Jun. 1999]; G. Conrau S. leg.; MfN URL: http://cool.mfn-berlin.de/u/d4c8af [MfN].

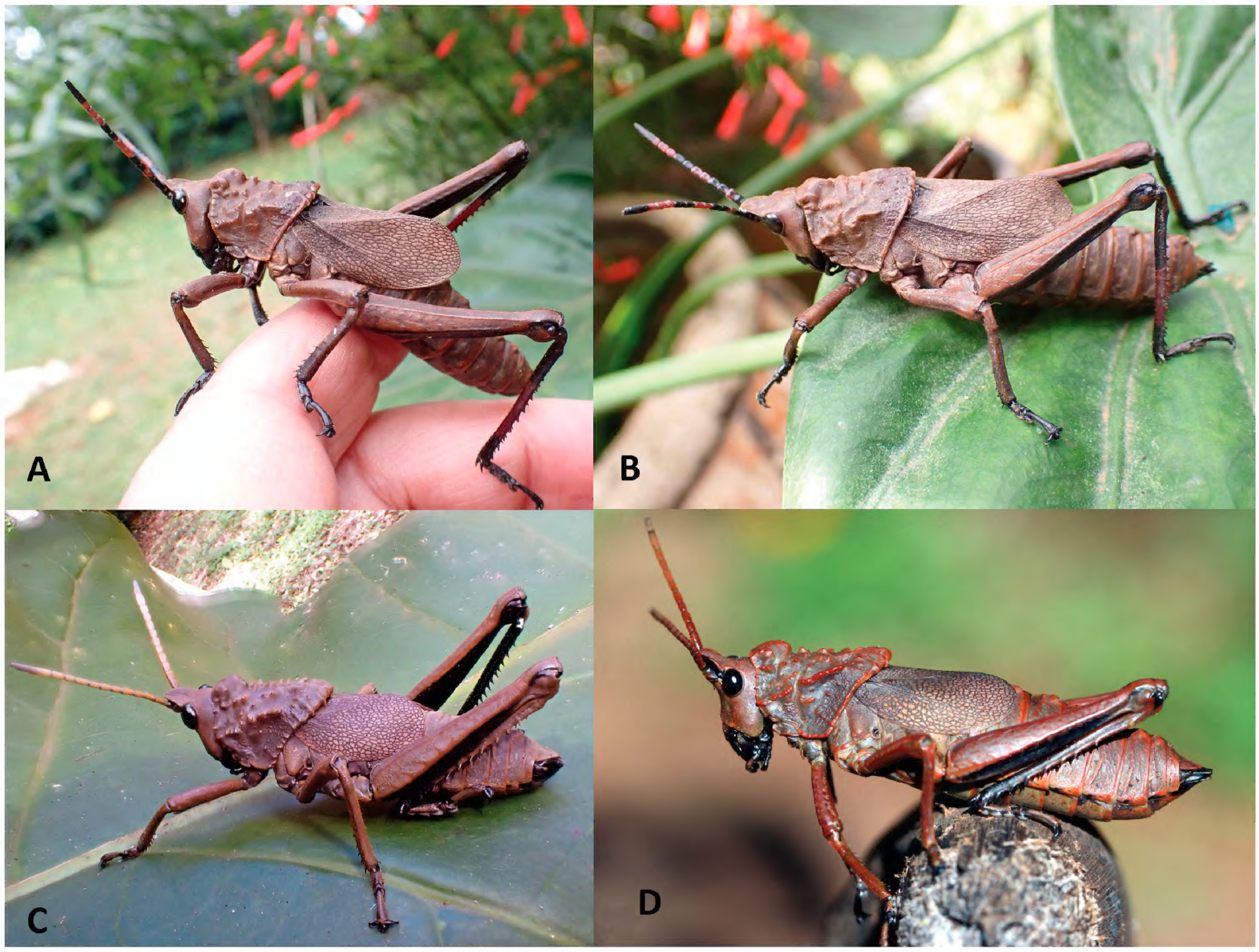

Figure 4. A, B. *L. tectiferus* sp. nov. **A.** Male; **B.** Female; **C, D.** *L. impotens*; **C.** Male; **D.** Female.

Material examined. Cameroon. • 1 male; Bamenda; Adametz S.G. leg.; URL: http://cool.mfn-berlin.de/u/bb659e (MfN). • 1 female; Bangwe; 1000 m; Mitte V–Mitte VI. 99 [mid-May.–mid-Jun. 1999]; G. Conrau S. leg.; URL: http://cool.mfn-berlin.de/u/d4c8af (MfN). • 1 female; Fotouni, West; 5.362°N, 10.246°E; 15 Jun. 2020; J.A. Yetchom Fondjo; SMNK; CMJ678. • 1 female; Fotouni, West; 5.362°N, 10.246°E; 13 Aug. 2020; J.A. Yetchom Fondjo leg.; SMNK; CMJ61. • 2 males, 2 females; Fotouni, West; 5.362°N, 10.246°E; 16 Jan. 2021; J.A. Yetchom Fondjo; SMNK; CMJ679. • 1 female; Fotouni, West; 5.362°N, 10.246°E; 14 Mar. 2022; J.A. Yetchom Fondjo; SMNK; CMJ63. • 2 females; Fotouni, West; 5.362°N, 10.246°E; 15 Mar. 2022; J.A. Yetchom Fondjo; SMNK; CMJ64.

Redescription. Male. ***Body*:** robust, depressed, with strongly rugose and tuberculated integument. ***Head*** (Fig. 2B, E, H): acutely conical; fastigium of vertex slightly curved upwards, flat, slightly concave in basal part, distinctly triangular and narrowing toward apex; antennae thick, shorter than head and pronotum together, with short transverse or subtransverse segments, the last apical segment being distinctly longer than others. ***Thorax*** (Fig. 2E, H): pronotum with large inflation in front of first sulcus, strongly and intensely rugose with more pointed tubercles; median carinae interrupted, lateral carinae absent; inferior margins of lateral lobes of pronotum straight; prozona shorter than metazona; posterior margin of metazona slightly emarginate in the middle; prosternal process very short, subacute; mesosternal interspace wider than long. ***Legs*** (Figs 1D, 2E, H): hind femur slender, its external area not expanded; upper-median margin of hind femora distinctly raised; obliquely expanded area at the base of hind femur strongly pronounced; external apical spine of hind tibiae present; hind tarsal segments not elongate. ***Elytra*** (Fig. 1D, 2E, H): less reticulated, shortened or brachypterous, oval, semilobed, reaching dorsally the third abdominal tergite, anterior margins rather curved, with very broadly rounded posterior margins. ***Abdomen*** (Figs 1D, 2E, H): often annulated; abdominal tergites each with a trigonal medio-dorsal tubercle; male subgenital plate compressed toward apex above, margins slightly incised, parallel; male supra-anal plate conical; male cerci (Fig. 7B) conical, straight. ***Epiphallus*** (Fig. 6B): bridge narrow, its anterior margin curved emarginate, posterior margin almost straight; anterior projections small; lateral plates oblique or divergent, its external margins fairly expanded; appendices of epiphallus narrow, subparallel, with apical lobes having only broader terminal processes, smaller processes absent, attached marginally to the basal part of external expansion of lateral plates, lying marginally to the external expansion of lateral plates; lophi very small or short, slightly curved,

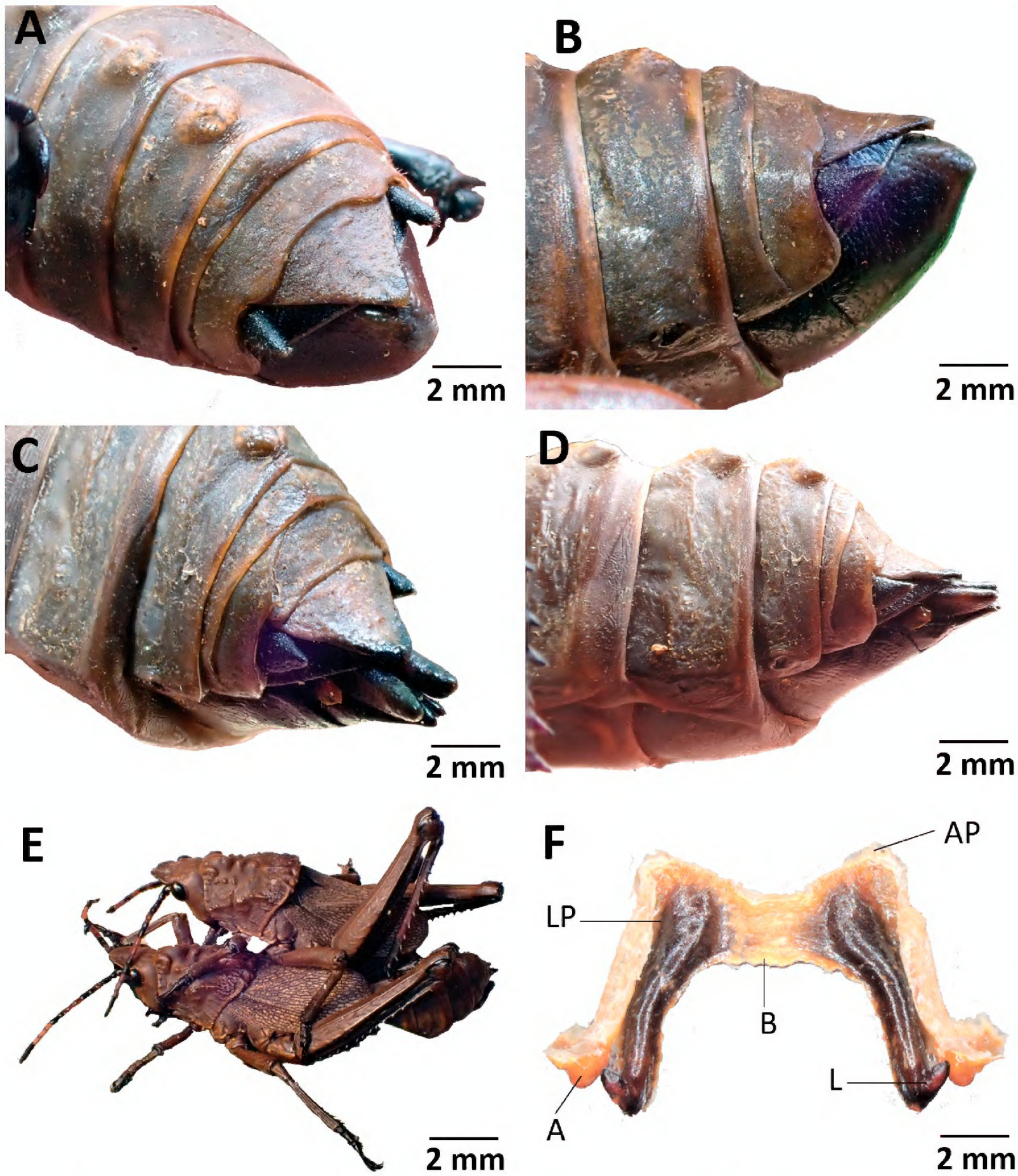

Figure 5. *L. tectiferus* sp. nov. **A.** Male semidorsal; **B.** Male in lateral view; **C.** Female semidorsal; **D.** Female in lateral view; **E.** *L. tectiferus* sp. nov. mating pair; **F.** Epiphallus.

and anteriorly directed with acute apex. ***Ectophallus*** (Fig. 6E, H, K): central membrane fairly narrow, subtriangular, marked at its lateral margins by furrows; zygoma broadly transverse, not extending halfway along the cingulum; suprazygomal plate rather U-shaped, slightly shorter than the zygoma; apodemal plates strongly produced ventrally, the apices fairly close to each other; valves of cingulum of smaller size, narrow, divergent in dorsal view; rami of cingulum narrow in dorsal view; dorsal cleft of cingulum large, ventral cleft narrow; suprarami well developed, large; sheats of moderate size, the inner margins separated from each other; ventral process of cingulum broadly triangular, slender, almost exceeding beyond endophallic apodemes in ventral view; basal emargination of cingulum very deep; ***Endophallus*** (Fig. 6E, H, K): endophallic apodemes of medium size, strongly produced forwards ventrally, exceeding beyond the basal emargination of cingulum; aedeagal valves small, short with button-like apices, with ventrolaterally directed process in its distal part; aedeagal sclerites narrow and of moderate size; pseudoarch small; spermatophore sac small, ovoid, not extending beyond the lateral limits of endophallic apodemes; gonopore at the middle.

Female. Similar to male but larger. ***Abdomen*** (Fig. 7E): ovipositor valves large, not sinuate; subgenital plate without carina, narrowed posteriorly, slightly emarginate at apex; egg guide prominent, conical, and slightly elongated; median longitudinal groove of genital chamber slender. ***Genitalia*** (Fig. 7H): spermatheca thick, lacking an apical pocket, with a laminated appearance in the apical part; spermatheca duct short, secondary diverticulum of spermathecal appendage of varying shape.

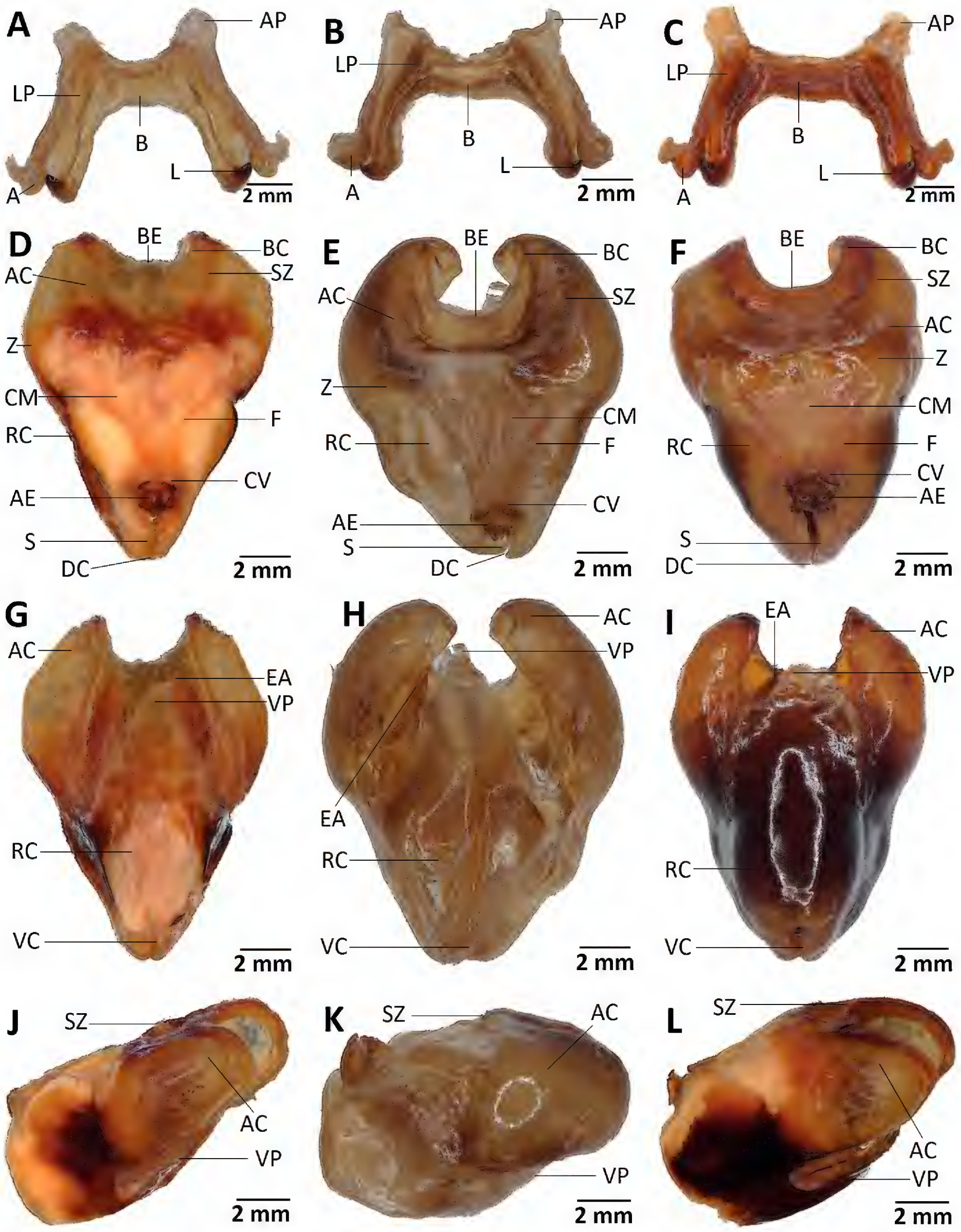

Figure 6. Phallic structures. **A–C.** Epiphallus dorsal view; **A.** *P. femorata*; **B.** *P. rammei*; **C.** *L. impotens*; **D–F.** Ectophallus + Endophallus dorsal view; **D.** *P. femorata*; **E.** *P. rammei*; **F.** *L. impotens*; **G–I.** Ectophallus + Endophallus ventral view; **G.** *P. femorata*; **H.** *P. rammei*; **I.** *L. impotens*; **J–L.** Ectophallus + Endophallus lateral view; **J.** *P. femorata*; **K.** *P. rammei*; **L.** *L. impotens*. A: appendices; AC: apodemal plate of cingulum; AE: aedeagus (aedeagal valves); AP: anterior projection of epiphallus; B: bridge of epiphallus; BC: basal thickening of cingulum; BE: basal emargination of cingulum; CM: central membrane of epiphallus; CV: valve of cingulum; DC: dorsal cleft of cingulum; EA: endophallic apodeme; F, marginal furrow separating suprarami and rami of cingulum; L: lophus of epiphallus; LP: lateral plate of epiphallus; RC: ramus of cingulum; S: sheath of ectophallus; SR: supraramus of cingulum; SZ: suprazygomal plate of cingulum; VC: ventral cleft of cingulum; VP: ventral process of cingulum; Z: zygoma of cingulum.

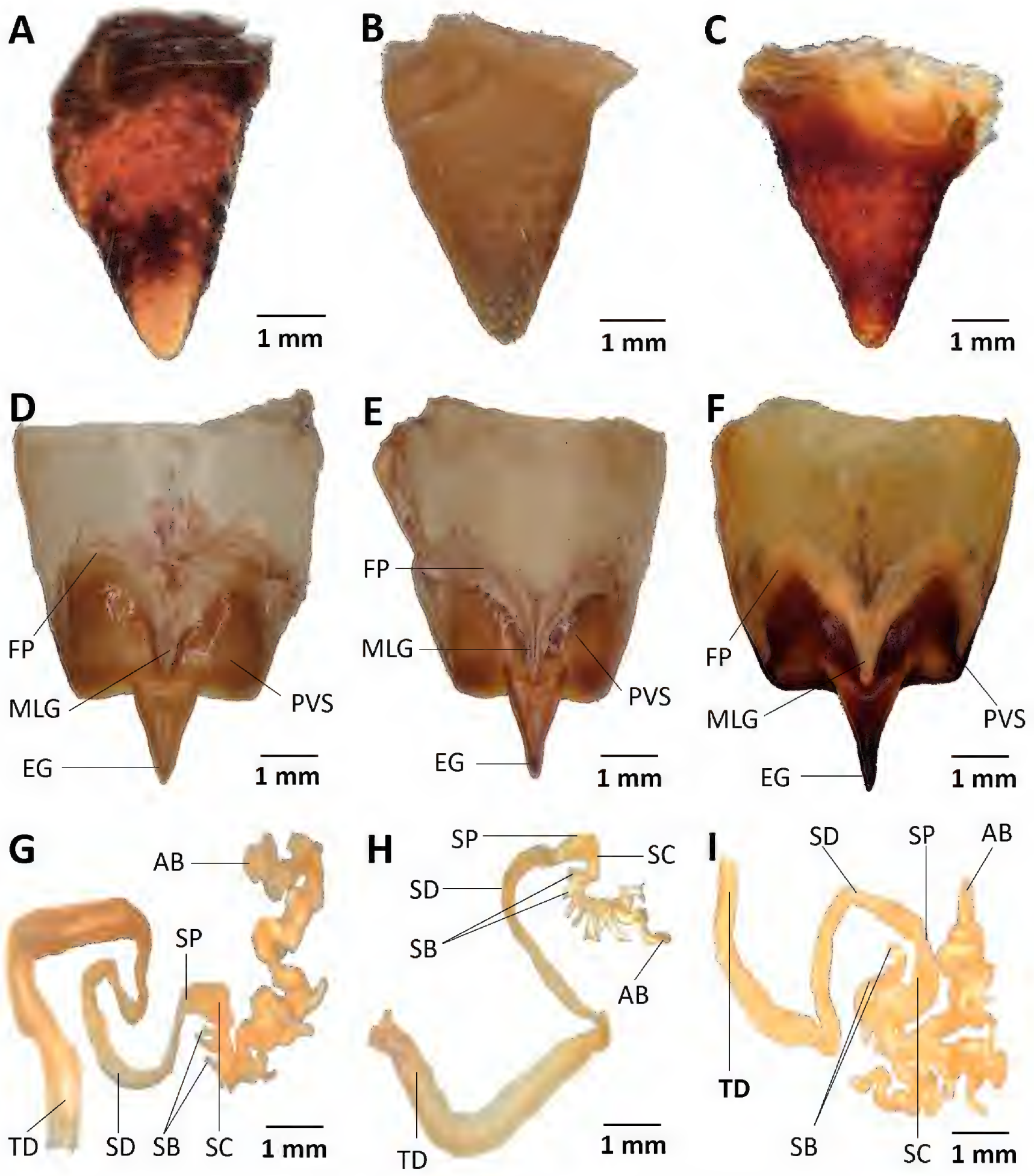

Figure 7. A–C. Male cerci; **A.** *P. femorata*; **B.** *P. rammei*; **C.** *L. impotens*; **D–F.** Female subgenital plates; **D.** *P. femorata*; **E.** *P. rammei*. **F.** *L. impotens*. **G–I.** Female spermatheca; **G.** *P. femorata*; **H.** *P. rammei*; **I.** *L. impotens*. AB: apical bulb of the spermathecal appendage; EG: egg-guide; FP: floor pouch of the female genital chamber; MLG: median longitudinal groove of the female genital chamber; PVS: postvaginal sclerite of the female genital chamber; SB: secondary diverticulum of the cecum of the spermatheca; SC: cecum of the spermatheca; SD: spermathecal duct; SP: spermathecal vesicle; TD: terminal dilatation of the spermathecal duct.

Color. Predominantly grayish; eyes red dark or entirely black in adults; labium, labrum, and mandibles red; hind knee entirely black in adults; elytra yellow-brown with brown veins; cerci yellowish or blackish; abdominal segments all separated by red lines; lower external, lower internal, mid internal, and upper internal hind femoral areas bright black.

Female. Pronotum testaceous brown with blood-like colored tubercles, more or less blackish below; antennae and legs reddish brown, more or less outlined with red; the outer-medial and upper-external area slightly variegated with yellowish brown, the margins more or less red, the tips of the femora black; hind tibiae all reddish brown, sometimes outlined with a blood-like color.

Male. Apex of antennae, apical 2/3 of hind tibiae, and ankles with blood-like colored tubercles; margin of vertex, lower part of antennae, fore and median femora, upper-external and medio-external areas of hind femora, anterior and median tibiae, and basal part of hind tibiae marked with yellow, especially on ribs.

Nymph with entirely black antennae, hind knees completely yellow.

Measurements. Male. Body length 32.83–35.37 mm; Female. Body length 43.22–49.73 mm. Adult individuals of *P. rammei* exhibit very large size variations in both sexes (Table 1).

Geographical distribution. *Parapetasia rammei* (as shown in Fig. 8) is limited to Cameroon. The species has been primarily observed in highland zones and grass fields, specifically in Bare-Dschang (the type locality), Bamenda, Bangwe, Fotouni, and Mt. Manengouba.

Ecology. *Parapetasia rammei* is typically associated with highland ecosystems. The species is commonly found on bare ground, low vegetation, and sometimes on shrubs in open vegetation, such as cultivated farms and fallows, as well as in steppe habitats. In its natural habitat, it can be observed throughout the year, with adults being particularly abundant during the rainy season. Nymphs are more commonly found during this period as well. Foamy secretions on tergites 7 and 8 are notable characteristics of the species and are also common in other pyrgomorphid species.

Key to the species of *Parapetasia*

1(2) Tegmina dark brown, strongly reduced, vestigial; first and/or second abdominal segments with a lateral black band behind the insertion points of the femora; anterior projections of epiphallus large; lateral plates subparallel; lophi large, strongly curved; suprazygomal plate widely rounded; apodemal lobes only slightly produced ventrally; basal emargination of cingulum shallow; endophallic apodemes short ..... *Parapetasia femorata* Bolívar, 1884 (Gabon, Cameroon, Equatorial Guinea, Nigeria)

2(1) Tegmina yellow-brown with brown veins, shortened or brachypterous, semilobed; first and/or second abdominal segments without a lateral black band behind the insertion points of the femora; anterior projections of epiphallus small; lateral plates oblique or divergent; lophi very small, slightly curved; suprazygomal plate U-shaped; apodemal lobes strongly produced ventrally; basal emargination of cingulum very deep; endophallic apodemes strongly elongate or slender ..... *Parapetasia rammei* Sjöstedt, 1923 (Cameroon)

Genus *Loveridgacris* Rehn, 1954

Parapetasia (*Loveridgea*) Rehn (1953)
Parapetasia (*Loveridgacris*) Rehn (1954)
Parapetasia (*Loveridgeacris*) Kevan (1962) (subsequent misspelling)
Parapetasia (*Loveridgacris*): Akbar & Kevan, (1964)

Diagnosis of the genus *Loveridgacris*. Fastigium of vertex rounded apically; tegmina brachypterous and slightly reticulated; eyes ovate and not prominent; posterior part of metazona not notably raised nor swollen, its median margin not emarginate; hind femora upper-median margin flat, not raised; male subgenital plate with fused margins; epiphallic bridge wide or broad; appendices divergent; ectophallus elongate; ventral process of cingulum subtriangular.

Loveridgacris impotens (Karsch, 1888)

Figs 1E, F; 2C, F, I, 3F, 4C, D, 6C, F, I, L, 7C, F, I

Petasia impotens Karsch, 1888
Parapetasia impotens Karsch

Holotype. Deutsch-Ostafrika [German East Africa]. • 1 male; Uzigna [Usegna]; MfN.

Synonyms. *Loveridgacris ulugurensis* Rehn (1953): 124, 126, pl. 2: f. 18 and 19, pl. 3: f. 23 and 24. Kevan et al. (1972): 223, 229.

Material examined. Deutsch-Ostafrika [German East Africa]. • 1 male; Uzigna [Usegna]; MfN. • 1 male; Amani; 26 Nov. 1906; S.G. Vosseler leg.; MfN. • 1 male; Amani; 1 Nov. 1906; S.G. Vosseler leg.; MfN. • 1 male, 1 female; Amani; Nov. 1906; Vosseler S.G. leg.; MfN. • 2 males; Amani; Nov. 1907; S.G. Vosseler leg.; MfN. • 1 female; Amani; 16 Jan. 1906; S.G. Vosseler leg.; MfN. • 1 male; Amani; 30 Nov.– 5 Dec.1906; S.G. Vosseler leg.; MfN. • 1 male; Amani; S.G. Vosseler leg.; MfN. • 1 male; Amani; 20 Nov.– 5 Dec. 1906; S.G. Vosseler leg.; MfN. • 1 male, 6 females, 1 nymph; Amani; S.G. Vosseler leg.; MfN. Tanzania. • 1 male; Uluguru-Berge; 11 Dec. 1998; S. Götze leg.; MfN. Deutsch-Ostafrika [German East Africa]. • 1 female; Sigital; Jul. 1903; S. Götze; MfN. • 1 female; Muoa, Bez.langa; S. Fischer; MfN. • 1 female; V. Karger leg.; MfN. • 2 males, 3 females; 1903, vend.1 Apr. 1911; Dr F. Eichelbaum; ZMH. Tanzania. • 1 female; Usambara Nguelo; S. Heinsen; MfN. • 1 female; Usambara Nguelo; 14 Jun. 1905; H. Rolle leg.; ZMH. Deutsch-Ostafrika [German East Africa]. • 4 males; 1908; S.G. Vosseler; MfN.

Redescription. Male. ***Body***: robust, depressed, with strongly rugose and tuberculated integument. ***Head*** (Fig. 1F, 2C, F, I): acutely conical; fastigium of vertex slightly curved upward, flat, slightly concave in basal part, with rounded apex in dorsal view; antennae thick, shorter than head and pronotum together, with short transverse or subtransverse segments, the last apical segment being distinctly longer than others; eyes oval, of moderate size. ***Thorax*** (Figs 2F, I, 3F, 4C, D): pronotum less testaceous, not deeply and concavely saddle-shaped, with large inflation in front of first sulcus, moderately rugose with slightly pointed tubercles; posterior part of metazonal disc not swollen or raised dorsally; median carinae interrupted, lateral carinae absent; lower margins of lateral lobes of

pronotum rather angular; prozona shorter than metazona; median posterior margin of metazona not emarginate; prosternal process very short, triangular, expanded at its base with angular apex; mesosternal interspace wider than long. ***Legs*** (Figs 2F, I, 3F, 4C, D): hind femur slender; upper-median margin of hind femora flat, not raised, almost of equal height to upper-external margin; obliquely expanded area at the base of hind femur less pronounced; external apical spine of hind tibiae present; hind tarsal segments not elongate. ***Elytra*** (Figs 1F, 2F, I, 4C, D): shortened or brachypterous, slightly elongated and strongly reticulated, reaching dorsally the third abdominal tergite, with evenly rounded posterior margins. ***Abdomen*** (Figs 2F, I, 3F, 4C, D): often annulated; abdominal tergites each with a trigonal medio-dorsal tubercle; male subgenital plate compressed toward apex above, margins fused but not separated; male supra-anal plate conical; male cerci conical (Fig. 7C). ***Epiphallus*** (Fig. 6C): bridge wide or broad, its anterior margin emarginate, and posterior margin almost straight; anterior projections large, fairly prominent; lateral plates almost divergent, its external margins slightly expanded; lophi of larger size, upcurved and anteriorly directed with acute apex; appendices divergent, with broad apical lobes bearing long terminal processes, attached submarginally to the anterior projections and lying close to the lateral plates. ***Ectophallus*** (Fig. 7F, I, L): elongate, stout; central membrane broad, marked at its lateral margins by furrows; zygoma narrow; suprazygomal plate narrow, slightly shorter than the zygoma, with rather widely rounded apex; apodemal plate broad and rounded in lateral view, lobes slightly produced ventrally, the apices fairly wide apart, without anterior blunt points; valves of cingulum of smaller size, divergent in dorsal view; rami of cingulum extending into sheath; sheath wide, inner margins fairly close to each other; dorsal cleft of cingulum large; ventral cleft of cingulum of moderate size; suprarami well developed, large; sheats well developed; ventral process of cingulum rather subtriangular, broadly covering the endophallic apodemes, slender, but not reaching or extending beyond endophallic apodemes in ventral view; basal emargination of cingulum shallow. ***Endophallus*** (Fig. 7F, I, L): endophallic apodemes moderately produced forward ventrally, rather broad, and reaching the basal emargination of cingulum; aedeagal valves of smaller size, broad, with button-like apices, and with ventrolaterally directed process in its distal part; aedeagal sclerites stout, slender, and curved; pseudoarch small, distinct, broad; spermatophore sac small, ovoid, extending beyond the lateral limits of endophallic apodemes; gonopore distally placed.

Female. As for male, but larger. ***Abdomen*** (Figs 4D, 7F): ovipositor valves large, not sinuate; subgenital plate without a carina, its posterior margin rounded and smooth; egg-guide prominent, conical, and highly elongated; median longitudinal groove of genital chamber slender. ***Genitalia*** (Fig. 7I): spermatheca thick, lacking an apical pocket, with a laminated appearance in the apical part; spermatheca duct slender, secondary diverticulum of spermathecal appendage of varying shape.

Color. General coloration brownish or reddish; eyes entirely black; head dark-red or brownish; labium, labrum, and mandible blackish; elytra light brown with dark-brown veins; lower-external, lower-internal, and medial-internal areas of hind femora blackish; hind tibiae sometimes brown in basal half and black in apical half.

Female. Antennae reddish brown; pronotum brown with dark-red tubercles; fore and middle femora, outer-medial, upper-external, and upper-internal areas of hind femora dark-red; fore and middle tibiae dark red; hind tibiae all brown in basal 2/3 and black in apical parts; tarsi blackish or dark-red; abdomen brownish; the posterior margins of the segments marked by red lines.

Male. Antenna light-brown; pronotum brownish with light-red tubercles in male; fore and middle femora, outer-medial, upper-external, and upper-internal areas of hind femora light-red; fore and middle tibiae light-red; hind tibiae all light-red in outer area and black in inner area; tarsi blackish or brownish.

Measurements. Male. Body length 50.88–60.19 mm; Female. Body length 48.72–63.69 mm. Adults of *L. impotens* exhibit significant size variation in both males and females. Table 1 provides detailed measurements of various body parts for this species.

Geographical distribution (Fig. 8). *Loveridgacris impotens* is a species that is found in East Africa. The species is known only from some of the Eastern Arc Mountains of Tanzania, on Zanzibar, and the Shimba Hills of Kenya.

Ecology. *Loveridgacris impotens* is a geophilous species found in lowland wet forests. The species produces the toxic foams (see the black arrow on Fig. 1F) by combining haemolymph with air through the spiracles.

Loveridgacris tectiferus Hemp, sp. nov.

https://zoobank.org/4A3C74E4-1002-458F-AC93-7F882AD0F4B5

Figs 3A–H, 4A, B, 5C, D

Holotype. Tanzania. • male; Udzungwa Mountains, Mang´ula; in disturbed lowland wet forest at border to National Park; Sep. 2022; Claudia Hemp leg.; Depository: CCH.

Paratypes. Tanzania. • 2 females; same data as for holotype. Depository: CCH.

Measurements. (mm) Males (n = 1): Body length: 51.20; Median length of pronotum: 13.60; length of hind femur: 25.00. Females (n = 2): Body length: 47.70–53.60; Median length of pronotum: 21.50–21.70; length of hind femur: 23.90–24.60.

Diagnosis. *Loveridgacris tectiferus* sp. nov. can be distinguished from *L. impotens* by the coloration of the antennae and hind tibiae. In *L. impotens*, the antennae are light or reddish brown, while in *L. tectiferus* sp. nov., segments alternate between black and orange (Fig. 4C, D). Similarly, the hind tibiae are uniformly brown and become darker at their apical parts in *L. impotens*, but are black with a median dull orange part in *L. tectiferus* sp. nov. The most noticeable difference between the two species is the shape of the tegmina, which are lobe-like and

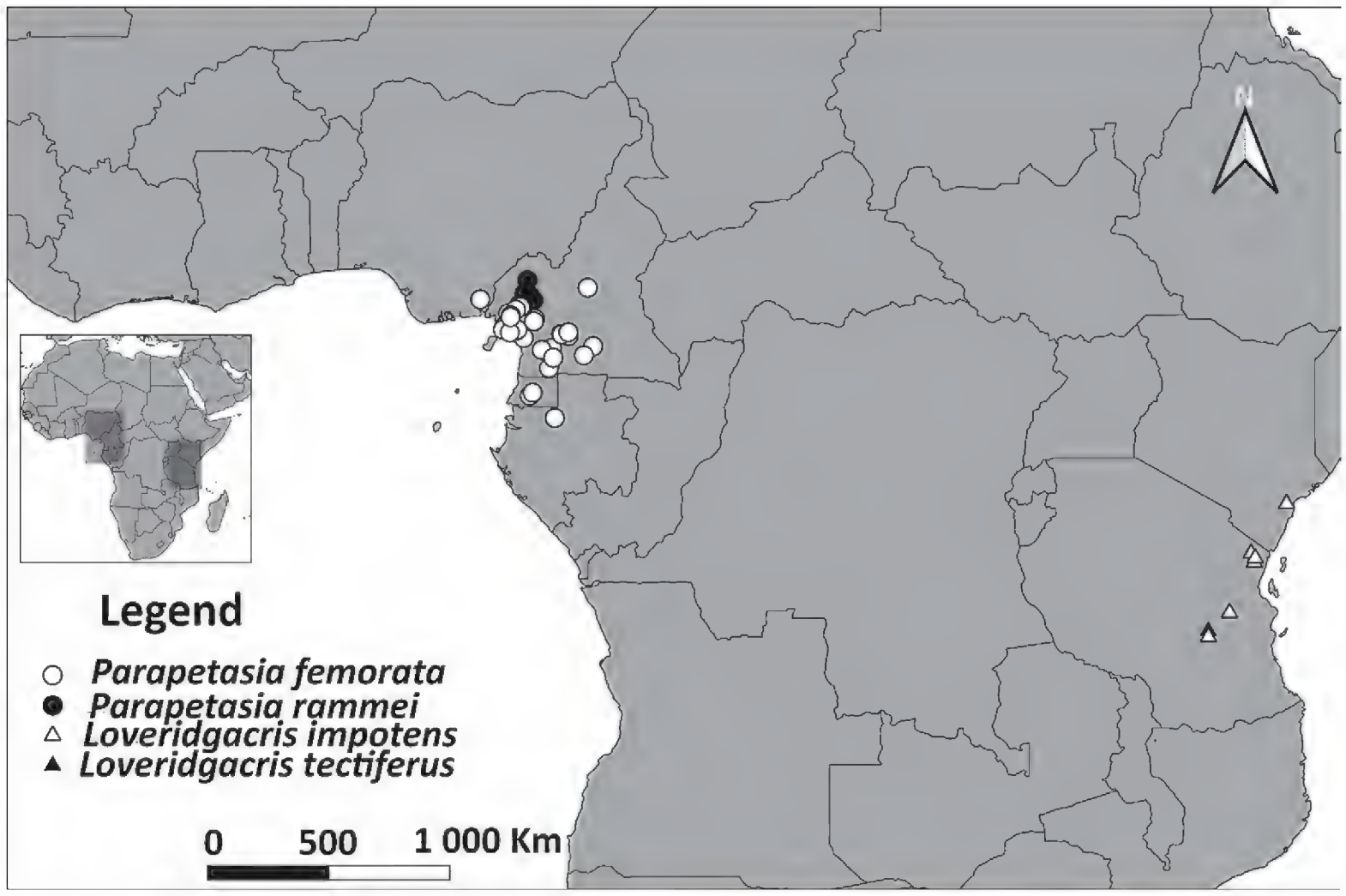

Figure 8. Geographical distribution of species in the genera *Parapetasia* and *Loveridgacris* (*P. femorata*, unfilled circle; *P. rammei*, filled circle; *L. impotens*, unfilled triangle; *L. tectiferus* sp. nov., filled triangle).

attached to the abdomen in *L. impotens*, while tectiform in *L. tectiferus* sp. nov. Both species are very similar in the overall shape of the head, pronotum, legs, and body, as well as in the tegminal pattern of darker veins on a light brown ground and their size. The epiphallus of both species is also very similar, consisting of hooked lophi and elongate appendices with bulbous end parts. However, in *L. tectiferus* sp. nov., the lophi are slender, and the hooks are slightly longer than those in *L. impotens*. Additionally, the appendices of the epiphallus are stouter in *L. impotens*, and the bridge of the epiphallus is slightly longer than that in *L. tectiferus* sp. nov. (see Fig. 5F and 6C for comparison).

Description. Male. ***General coloration.*** Overall, color brown with antennae with conspicuously black and orange colored segments. Eyes and labrum black. Hind femora ventrally black, hind tibiae black with dull orange middle part (Fig. 4A). ***Head and antennae.*** Antennae thick, rod-like with basal segments black, and then alternating one or two segments orange and black (Fig. 3A, C). Antennae slightly shorter than head and pronotum together. Fastigium of vertex upcurved, slightly concave in the middle, with acute-angular apex. Frons incurved. Frontal ridge narrow, constricted between antennae (Fig. 3A). ***Pronotum and wings.*** Pronotum in front of first sulcus with large hump, remaining pronotum strongly rugose with elevated ridges and tubercles. Median carina irregular, obtuse, lateral carinae absent. Posterior margin of pronotum with ridge-like tubercles along the edge. Prosternal process low, subpyramidal. Mesosternal interspace wider than long, with deep grooves (Fig. 3E). Tegmina tectiform, shortened, slightly exceeding abdominal segment 3. Hind wings absent. ***Abdomen.*** All abdominal segments with dorsal tubercles. Male supra-anal plate triangular (Fig. 5A), cerci laterally compressed, black, with blunt apex. Subgenital plate obtusely conical (Fig. 5B). Internal morphology. Epiphallus typical for Dictyophorini. Lophi of epiphallus strongly sclerotized with well-developed dorsolaterally directed apical hooks. Appendix of the epiphallus with angular externolateral sclerotized processes running parallel to the lophi; apices knob-like with ventral directed dent. Bridge little sclerotized and comparatively narrow.

Female. Larger and stouter than the male, with the same coloration as male; predominantly brown with antennae with black and orange segments, black eyes, and labrum. Underside of hind femora black, hind tibia black with median dull orange part (Fig. 4B). Antennae, head, and pronotum as male. Supra-anal plate triangular with blunt apex (Fig. 5C). Cerci laterally compressed, black (Fig. 5C, D). Ovipositor valves black, straight, rounded, with blunt apices (Fig. 5C, D).

Etymology. From Latin: *-tectum* = roof, because of the tectiform-shaped tegmina.

Habitat. A geophilous species of lowland wet forest.

Ecology. In captivity, individuals have the same preference for monocotyledonous plants as observed for *Dictyophorus griseus* (Rowell et al. 2015). Even when offered various other plants, they preferred to feed on Liliaceae leaves and flowers. Mating took approximately half an hour, and the male sat on top of the female, bending its abdomen under that of the female for copulation (Fig. 5E). Even when roughly handled, no reflex bleeding was observed, as is common in other Dictyophorini species and also observed in *L. impotens* (Fig. 1F).

Nymphs. Unknown but are probably similar to nymphs of *L. impotens* (Fig. 1E).

Distribution. Tanzania, Udzungwa Mountains.

Key to the species of *Loveridgacris*

1(2) Antennae light or reddish brown; hind tibiae uniformly brown, their apical parts darker; tegmina lobe-like and attached to the abdomen (Fig. 4C, D) ..... *Loveridgacris impotens* (Karsch, 1888) (Tanzania, Kenya)

2(1) Antennal segments alternate between black and orange; hind tibiae black with a median dull orange part; tegmina tectiform (Fig. 4A, B) ..... *Loveridgacris tectiferus* Hemp, sp. nov. (Tanzania)

Phylogenetic analysis

In total, 47 DNA barcode sequences belonging to 10 Pyrgomorphidae species were analyzed. The locations of collection of the samples used are presented in Table 4. For the genera *Parapetasia* and *Loveridgacris*, two species representing all known species were analyzed. Six additional species defined as outgroups included *Zonocerus elegans* (Thunberg, 1815), *Phyteumas purpurascens* (Karsch, 1896), *Phymateus viridipes* (Stål, 1873), *Taphronota calliparea calliparea* (Schaum, 1853), *Dictyophorus spumans* (Thunberg, 1787), and *Dictyophorus griseus* (Reiche & Fairmaire, 1849). One phylogenetic tree based on the concatenated sequence alignments of the two individual gene datasets (COI = 565 bp, 16S = 376 bp) was constructed with the BI method (Fig. 9). The concatenated sequence alignment included 941 bp. The most basal clusters of the phylogenetic tree comprised the subtribes Zonocerina (*Zonocerus*), Phymateina (*Phymateus*, *Phyteumas*), and Taphronotina (*Taphronota*). The tribes Taphronotini and Phymateini were well resolved, and all members of these tribes clustered together; similarly, members of the subtribes Zonocerina and Phymateina were well resolved. The tribe Dictyophorini represented a separate clade relative to Taphronotini and Phymateini. The tribe Dictyophorini was divided into three groups, representing three different genera. We found strong support for the monophyly of the genera *Loveridgacris*, *Parapetasia*, and *Dictyophorus*. The species tree inferred using the BI approach (Fig. 9) clustered. *Loveridgacris* near *Parapetasia* with high posterior probability support (score > 0.95). The cluster, including only the members of *Parapetasia*, was divided into two groups, and *Parapetasia rammei* was the sister to *Parapetasia femorata*. Both had relatively large interspecific distances (3.75%). The two *Loveridgacris* species (*L. impotens* and *L. tectiferus* sp. nov.) showed substantial sequence divergence from the other genera. The distances between *L. impotens* and *P. femorata* (6.70%) and between *L. impotens* and P. *rammei* (7.58%) were relatively large. At the species level, *L. impotens* and *L. tectiferus* sp. nov. are not completely resolved, but *L. tectiferus* sp. nov. is monophyletic with high support; the species show low genetic distance (0.33%).

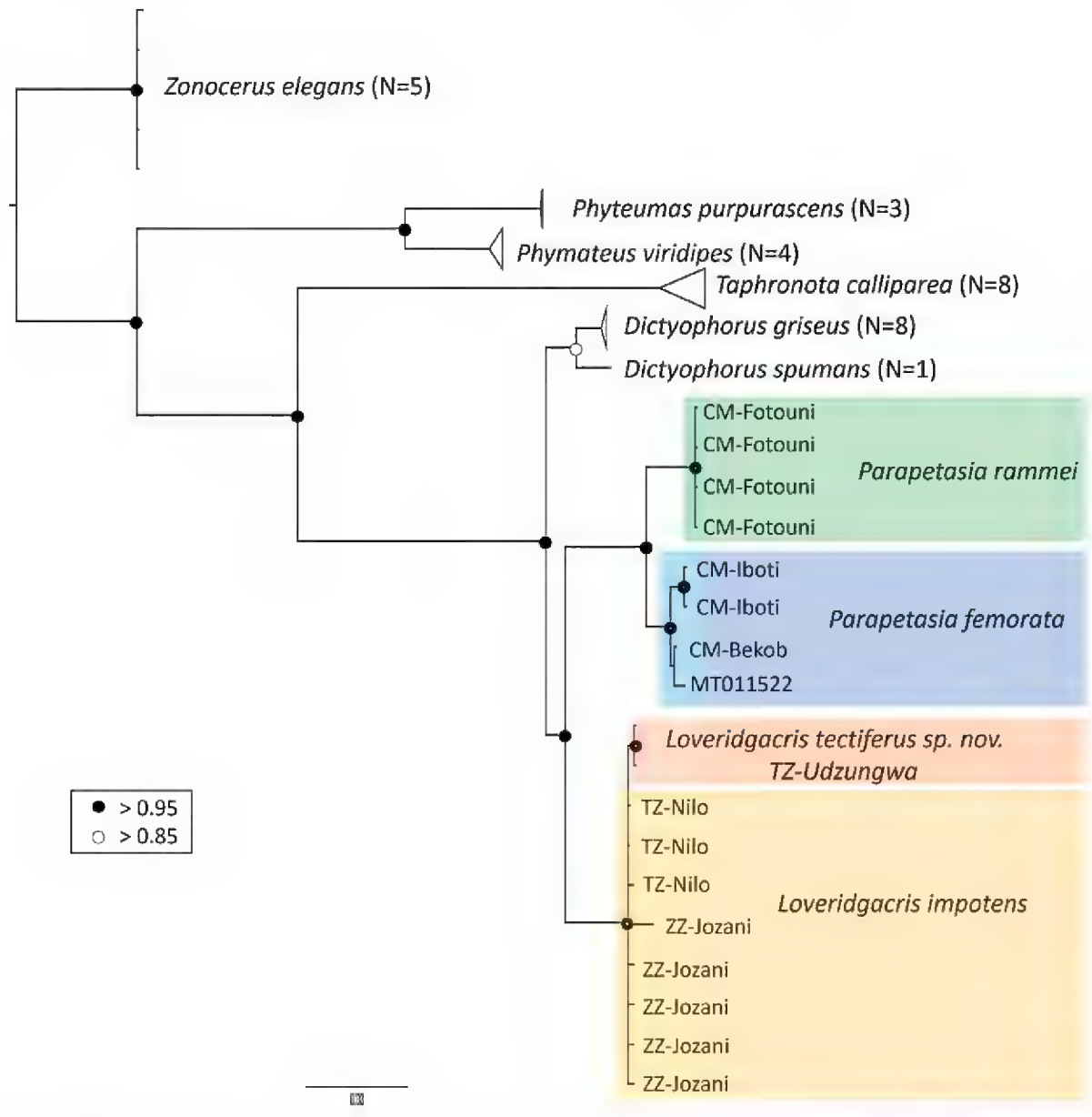

Figure 9. Bayesian inference (BI) tree built from the concatenated sequence alignment of mtDNA COI/16S gene fragments. The Bayesian posterior probabilities (PPs) are shown close to the nodes.

Mitochondrial genome organization, structure, and base composition in *Loveridgacris*

The mitogenomes of *Loveridgacris impotens* and *Loveridgacris tectiferus* sp. nov. are 15,592 bp and 15,737 bp long, respectively (see Suppl. 1). Both are organized in the typical metazoan mitochondrial gene set consisting of 37 genes, namely, 13 protein-coding genes, 22 transfer RNA genes, two ribosomal RNA genes (rrnL and rrnS), and one A+T-rich control region (Table 2). A comparison of the whole mitogenomes, rrnL genes, rrnS genes, and A+T-rich regions of *L. impotens* and *L. tectiferus* sp. nov. are shown in Table 4. The nucleotide composition of the entire mitochondrial genome of both species is A+T-biased, with contents ranging from 70.0% in *L. impotens* to 74.1% in *L. tectiferus* sp. nov. (Table 3). The skew metrics of the protein-coding genes within *L. impotens* and *L. tectiferus* sp. nov. showed a positive AT-skew and a negative GC-skew, indicating that base C was more abundant than base G in the mitogenomes of both species (Table 3).

The pairwise genetic distances (see Suppl. 2) inferred from all 13 protein-coding genes showed that the interspecies genetic distance ranged from 0% (ATP8) to 0.8% (ND4), indicating relatively low genetic distances between *L. impotens* and *L. tectiferus* sp. nov., regardless of the gene considered. Among the 13 PCGs, ND2, COI, COII, ATP8, ATP6, COIII, ND3, and ND6 CYTB were encoded on the majority strand (J-strand), while ND1, ND4, ND4L, and ND5 were encoded on the minority strand (N-strand) (Table 2). Transfer RNA genes are located on the J strand, except for tRNA-Gln, tRNA-Cys, tRNA-Tyr, tRNA-Phe, tRNA-His, tRNA-Pro, tRNA-Leu1, and tRNA-Val, which are located on the N strand (Table 2). Most of the PCGs (ND2, COII, ATP6, COIII, ND4L, ND6, and CYTB) have ATG as the start codon; ATP8 has ATC as the start codon; COI has ACT as the start codon; ND3 and ND5 have ATT as the start codon, and ND1 has ATA as the start codon. All PCGs use complete TAA as the stop codon, except COIII, ND5, and ND4, which use ACT, ATT, and TAG, respectively, as the stop codon (Table 2).

Table 2. Distribution of protein-coding genes (PCGs), transfer RNA genes, ribosomal RNA genes, and A+T-rich regions in the mitogenome of *Loveridgacris* impotens.

Species	*Loveridgacris impotens*					
Genes	**Length (bp)**	**Position**	**Start codon**	**Stop codon**	**Strand**	**Anticodon**
ND2	1,023	197–1219	ATG	TAA	J	
COX1	1545	1415–2959	ACT	TAA	J	
COX2	684	3029–3712	ATG	TAA	J	
ATP8	159	3858–4016	ATC	TAA	J	
ATP6	678	4010–4687	ATG	TAA	J	
COX3	820	4694–5513	ATG	ACT	J	
ND3	354	5548–5901	ATT	TAA	J	
ND5	1717	6311–8027	ATT	ATT	N	
ND4	1335	8112–9446	GTG	TAG	N	
ND4L	294	9440–9733	ATG	TAA	N	
ND6	522	9871–10392	ATG	TAA	J	
CYTB	1143	10396–11538	ATG	TAG	J	
ND1	945	11625–12569	ATA	TAG	N	
tRNA-Ile	64	1–64	AAT	TAA	J	GAT
tRNA-Gln	69	62–130			N	TTG
tRNA-Met	67	130–196			J	CAT
tRNA-Trp	71	1224–1294			J	TCA
tRNA-Cys	63	1287–1349			N	GCA
tRNA-Tyr	69	1354–1422			N	GTA
tRNA-Leu2	65	2955–3019			J	TAA
tRNA-Asp	64	3711–3774			J	GTC
tRNA-Lys	71	3775–3845			J	CTT
tRNA-Gly	64	5484–5547			J	TCC
tRNA-Ala	66	5902–5967			J	TGC
tRNA-Arg	65	5967–6031			J	TCG
tRNA-Asn	68	6043–6110			J	
tRNA-Ser	70	11537–11606			J	TGA
tRNA-Glu	64	6184–6247			J	TTC
tRNA-Phe	64	6246–6309			N	GAA
tRNA-His	70	8043–8112			N	GTG
tRNA-Thr	68	9736–9803			J	TGT
tRNA-Pro	65	9804–9868			N	TGG
tRNA-Ser2	68	6111–6178			J	GCT
tRNA-Leu1	65	1273–12637			N	TAG
tRNA-Val	68	13939–14006			N	TAC
L-rRNA	1252	13897–12646			J	
S-rRNA	785	14017–14801			N	
A+T-rich region	791	14802–15592			J	N/A

Table 3. Nucleotide composition of the complete mitogenome for each *Loveridgacris* species examined.

Species		*Loveridgacris impotens*	*Loveridgacris tectiferus* sp. nov.
Accession number		OR730795	OR730794
Length (bp)		15592	15737
Whole mitogenome	A	6869 (40.0%)	6947 (44.1%)
	T	4679 (30.0%)	4709 (29.9%)
	G	1539 (9.9%)	1543 (9.8%)
	C	2507 (16.1%)	2538 (16.1%)
	A+T	11546 (70.0%)	11656 (74.1%)
	G+C	4046 (26.0%)	4081 (25.9%)
	AT-skew	0.14	0.19
	GC-skew	-0.24	-0.24

Discussion

Taxonomy

This study was conducted to investigate the genera *Parapetasia* and *Loveridgacris* using a combination of morphological, distributional, and molecular data. *Parapetasia rammei* has been used by Seino and Njoya (2018); hence, this name is currently considered valid in the OSF (Cigliano et al. 2023). In this study, *Parapetasia rammei* was formally resurrected.

We present herein the description of a new species, *Loveridgacris tectiferus* sp. nov., discovered in Tanzania. Despite exhibiting distinguishable morphological traits, our genetic analysis reveals minimal differences between *Loveridgacris tectiferus* sp. nov. and *L. impotens*. This suggests that *Loveridgacris tectiferus* sp. nov. is likely a recently evolved species, indicative of its youth within the taxonomic hierarchy. Indeed, *L. impotens* and

Table 4. Taxon sampling and GenBank accession numbers.

Species	Country	Locality	Specimen codes	GenBank Accession number		GenSeq Nomenclature	References
				COI	16S		
Dictyophorus griseus (Reiche & Fairmaire, 1849)	Cameroon	Fotouni	CMJ65 (non-type specimen voucher)	OR583878	PP552786	genseq-4 COI, 16S	This study
Dictyophorus griseus (Reiche & Fairmaire, 1849)	Cameroon	Fotouni	CMJ66 (non-type specimen voucher)	OR583879	PP552787	genseq-4 COI, 16S	This study
Dictyophorus griseus (Reiche & Fairmaire, 1849)	Cameroon	Fotouni	CMJ67 (non-type specimen voucher)	OR583880	PP552788	genseq-4 COI, 16S	This study
Dictyophorus griseus (Reiche & Fairmaire, 1849)	Cameroon	Fotouni	CMJ70 (non-type specimen voucher)	OR583881	PP552789	genseq-4 COI, 16S	This study
Dictyophorus griseus (Reiche & Fairmaire, 1849)	Cameroon	Fotouni	CMJ72 (non-type specimen voucher)	OR583882	PP552790	genseq-4 COI, 16S	This study
Dictyophorus griseus (Reiche & Fairmaire, 1849)	Cameroon	Fotouni	CMJ814 (non-type specimen voucher)	OR583885	PP552791	genseq-4 COI, 16S	This study
Dictyophorus griseus (Reiche & Fairmaire, 1849)	Cameroon	Fotouni	CMJ816 (non-type specimen voucher)	OR583886	PP552792	genseq-4 COI, 16S	This study
Dictyophorus griseus (Reiche & Fairmaire, 1849)	Cameroon	Fotouni	CMJ817 (non-type specimen voucher)	OR583887	PP552793	genseq-4 COI, 16S	This study
Dictyophorus spumans (Thunberg, 1787)	South Africa	Western Cape	ORTH48 (non-type specimen voucher)	NA	PP552794	genseq-4 16S	This study
Loveridgacris impotens (Karsch, 1888)	Tanzania	Nilo	TZC1351 (non-type specimen voucher)	NA	PP552822	genseq-4 16S	This study
Loveridgacris impotens (Karsch, 1888)	Tanzania	Nilo	TZC1379 (non-type specimen voucher)	OR578932	PP552823	genseq-4 COI, 16S	This study
Loveridgacris impotens (Karsch, 1888)	Tanzania	Nilo	TZC1380 (non-type specimen voucher)	NA	PP552824	genseq-4 16S	This study
Loveridgacris impotens (Karsch, 1888)	Tanzania	Nilo	TZC1381 (non-type specimen voucher)	OR578933	NA	genseq-4 COI	This study
Loveridgacris impotens (Karsch, 1888)	Zanzibar	Jozani	ZZC1434 (non-type specimen voucher)	NA	PP552980	genseq-4 16S	This study
Loveridgacris impotens (Karsch, 1888)	Zanzibar	Jozani	ZZC1435 (non-type specimen voucher)	NA	PP552825	genseq-4 16S	This study
Loveridgacris impotens (Karsch, 1888)	Zanzibar	Jozani	ZZC1436 (non-type specimen voucher)	NA	PP552826	genseq-4 16S	This study
Loveridgacris impotens (Karsch, 1888)	Zanzibar	Jozani	ZZC1437 (non-type specimen voucher)	NA	PP552827	genseq-4 16S	This study
Loveridgacris impotens (Karsch, 1888)	Zanzibar	Jozani	ZZC1438 (non-type specimen voucher)	NA	PP552828	genseq-4 16S	This study
Loveridgacris tectiferus sp. nov.	Tanzania	Udzungwa	TZC1336 (holotype)	OR730794	PP552820	genseq-1 COI, 16S	This study
Loveridgacris tectiferus sp. nov.	Tanzania	Udzungwa	TZC1352 (paratype)	OR583893	PP552821	genseq-2 COI, 16S	This study
Parapetasia femorata Bolívar, 1884	NA	NA	NA	MT011522	NA	genseq-4 COI	Song et al. (2020)
Parapetasia femorata Bolívar, 1884	Cameroon	Iboti	CMJ244 (non-type specimen vouvher)	OR583883	PP552818	genseq-4 COI, 16S	This study
Parapetasia femorata Bolívar, 1884	Cameroon	Iboti	CMJ245 (non-type specimen vouvher)	OR578931	PP552979	genseq-4 COI, 16S	This study
Parapetasia femorata Bolívar, 1884	Cameroon	Bekob	CMJ598 (non-type specimen vouvher)	OR583884	PP552819	genseq-4 COI, 16S	This study
Parapetasia rammei Sjöstedt, 1923	Cameroon	Fotouni	CMJ61 (non-type specimen vouvher)	OR583875	PP552814	genseq-4 COI, 16S	This study
Parapetasia rammei Sjöstedt, 1923	Cameroon	Fotouni	CMJ62 (non-type specimen voucher)	OR583876	PP552815	genseq-4 COI, 16S	This study
Parapetasia rammei Sjöstedt, 1923	Cameroon	Fotouni	CMJ63 (non-type specimen voucher)	OR578930	PP552816	genseq-4 COI, 16S	This study
Parapetasia rammei Sjöstedt, 1923	Cameroon	Fotouni	CMJ64 (non-type specimen voucher)	OR583877	PP552817	genseq-4 COI, 16S	This study
Phymateus viridipes (Stål, 1873)	Tanzania	Nguru	TZC1339 (non-type specimen voucher)	NA	PP552803	genseq-4 16S	This study
Phymateus viridipes (Stål, 1873)	Tanzania	Nguru	TZC1340 (non-type specimen voucher)	OR583890	PP552804	genseq-4 COI, 16S	This study
Phymateus viridipes (Stål, 1873)	Tanzania	Nguru	TZC1354 (non-type specimen voucher)	NA	PP552805	genseq-4 16S	This study
Phymateus viridipes (Stål, 1873)	Tanzania	Nguru	TZC1355 (non-type specimen voucher)	OR583894	PP552806	genseq-4 COI, 16S	This study
Phyteumas purpurascens (Karsch, 1896)	Tanzania	Nguru	TZC1343 (non-type specimen voucher)	OR583892	PP552807	genseq-4 COI, 16S	This study
Phyteumas purpurascens (Karsch, 1896)	Tanzania	Wikwescho	TZC1388 (non-type specimen voucher)	OR578937	PP552808	genseq-4 COI, 16S	This study
Phyteumas purpurascens (Karsch, 1896)	Tanzania	Wikwescho	TZC1389 (non-type specimen voucher)	OR578938	PP552809	genseq-4 COI, 16S	This study

Species	Country	Locality	Specimen codes	GenBank Accession number		GenSeq Nomenclature	References
				COI	16S		
Taphronota calliparea (Schaum, 1853)	Tanzania	Kimboza	TZC1335 (non-type specimen voucher)	OR583888	PP552795	genseq-4 COI, 16S	This study
Taphronota calliparea (Schaum, 1853)	Tanzania	Nguru	TZC1341 (non-type specimen voucher)	NA	PP552796	genseq-4 16S	This study
Taphronota calliparea (Schaum, 1853)	Tanzania	Nguru	TZC1342 (non-type specimen voucher)	OR583891	PP552797	genseq-4 COI, 16S	This study
Taphronota calliparea (Schaum, 1853)	Tanzania	Nilo	TZC1383 (non-type specimen voucher)	OR583895	PP552798	genseq-4 COI, 16S	This study
Taphronota calliparea (Schaum, 1853)	Tanzania	Nilo	TZC1384 (non-type specimen voucher)	OR583896	PP552799	genseq-4 COI, 16S	This study
Taphronota calliparea (Schaum, 1853)	Tanzania	Nilo	TZC1385 (non-type specimen voucher)	OR578934	PP552800	genseq-4 COI, 16S	This study
Taphronota calliparea (Schaum, 1853)	Tanzania	Nguru	TZC1386 (non-type specimen voucher)	OR578935	PP552801	genseq-4 COI, 16S	This study
Taphronota calliparea (Schaum, 1853)	Tanzania	Nguru	TZC1387 (non-type specimen voucher)	OR578936	PP552802	genseq-4 COI, 16S	This study
Zonocerus elegans (Thunberg, 1815)	Tanzania	Nguru	TZC1337 (non-type specimen voucher)	NA	PP552810	genseq-4 16S	This study
Zonocerus elegans (Thunberg, 1815)	Tanzania	Nguru	TZC1338 (non-type specimen voucher)	OR583889	PP552811	genseq-4 COI, 16S	This study
Zonocerus elegans (Thunberg, 1815)	Tanzania	Nilo	TZC1390 (non-type specimen voucher)	NA	PP552812	genseq-4 16S	This study
Zonocerus elegans (Thunberg, 1815)	Tanzania	Nilo	TZC1391 (non-type specimen voucher)	OR578939	PP552813	genseq-4 COI, 16S	This study
Zonocerus elegans (Thunberg, 1815)	–		–	MT011544	NA	genseq-4 COI, 16S	Song et al. (2020)

L. tectiferus sp. nov. inhabit different mountain habitats in Tanzania, with *L. impotens* being widely distributed, while *L. te*ctiferus is restricted to Udzungwa mountain so far. This suggests a possibility of sympatric speciation due to habitat isolation, which may cause disruption of gene flow. Our findings align with prior investigations of Orthopteran taxa, particularly those inhabiting the Eastern Arc Mountains. These studies indicate that while genera within this region have ancient origins, speciation at the species level appears to be relatively young. This pattern is attributed to historical climatic fluctuations, which have intermittently fragmented and interconnected habitats, facilitating both isolation and subsequent diversification. Similar mechanisms have been documented in various Orthopteran groups, including Lentulidae (Hemp et al. 2020), the coptacrine genus *Parepistaurus* (Hemp et al. 2015), the hexacentrine genus *Aerotegmina* (Grzywacz et al. 2021), and the meconematine genus *Amytta* (Hemp et al. 2018). These studies collectively underscore the dynamic interplay between historical environmental factors and evolutionary processes, shaping the diversity of Orthopteran fauna in the Eastern Arc Mountains and beyond. Two species are now included in both *Parapetasia* (*P. femorata* and *P. rammei*) and *Loveridgacris* (*L. impotens* and *Loveridgacris tectiferus* sp. nov.).

Akbar and Kevan (1964) used external morphology and phallic structures to distinguish between the genera *Parapetasia* and *Loveridgacris*. Although they did not examine the phallic structures of *P. rammei*, they concluded that *Parapetasia* has an epiphallus with subparallel lateral plates and appendices, a triangular fastigium of the vertex, and other anatomical features similar to those of *P. femorata*. However, the phallic structures of *P. rammei*, as illustrated in this study, reveal that the epiphallus has a narrow bridge but divergent lateral plates, resembling those of *Loveridgacris* rather than *Parapetasia*.

Akbar and Kevan (1964) noted that *Parapetasia* species, specifically *P. femorata*, have epiphallus appendices with smaller and broader terminal processes. However, *P. rammei* has appendices with broader terminal processes and lacks smaller terminal processes. The bridge of the epiphallus is also longer in *P. rammei* than in *P. femorata*. Additionally, our findings indicate that the lophi in *P. rammei* are smaller than those in *Loveridgacris*, contradicting Akbar and Kevan's claim that *Loveridgacris* has small lophi.

According to Kevan et al. (1974), *P. calabarica* and *P. rammei* are likely variations of *P. femorata* with smaller wings. Later, Kevan (1977) combined all three species into *P. femorata* based on their shared geographic range and morphological similarities. However, DNA evidence and differences in external morphology and phallic structures show that *P. femorata* and *P. rammei* are distinct species. Therefore, *P. rammei* should be recognized as a separate species within the genus *Parapetasia*.

The present study highlights the importance of combining multiple sources of information and DNA markers for the identification of Afrotropical grasshopper species of the genera *Parapetasia* and *Loveridgacris*.

Distribution

The type specimen of *P. rammei* was found in Bare-Dschang, a high-altitude location in western Cameroon. Two specimens at MfN labeled holotype (male) and allotype (female) were actually paratypes and collected from Bamenda and Bangwe in the northwestern region

of Cameroon. The true holotype, a female specimen, is housed in the Stockholm Museum. Seino and Njoya (2018) also collected *P. rammei* from the northwestern region of Cameroon, which is known for its high altitude. We found *P. rammei* in Fotouni in the western highlands and in the steppe habitats of the Manengouba Mountains. Our observations are supported by Rehn (1953), who suggested that *P. rammei* is limited to the highest areas of Cameroon. Our research, together with museum data, indicates that *P. femorata* inhabits forested areas in Western and Central African countries such as Cameroon, Equatorial Guinea, Gabon, and Nigeria. Although the species is widespread in Cameroon, its distribution in neighboring countries may be underestimated due to a lack of sampling. Hence, our results show that *P. femorata* and *P. rammei* occupy different ecological niches.

Loveridgacris impotens and *L. tectiferus* sp. nov. are found only in Tanzania and Kenya. Therefore, the genus *Parapetasia* is restricted to western and central Africa, while *Loveridgacris* is exclusive to East Africa. The new species *L. tectiferus* has to be considered a narrow range endemic, whereas *L. impotens* is widespread in eastern Africa.

Phylogeny

Although *Parapetasia* and *Loveridgacris* have been the subject of taxonomic discussions since I. Bolívar (1884), their taxonomy and systematic status have remained complex and challenging; thus, we provide the first attempt at a molecular phylogeny for the tribe Dictyophorini.

Our results divided the studied Pyrgomorphidae into three main tribes (Dictyophorini, Phymateini, and Taphronotini). Taphronotini, which includes a single species, *Taphronota calliparea*, is closely related to Dictyophorini, which includes three genera (*Dictyophorus*, *Loveridgacris*, and *Parapetasia*). In addition, the genera *Zonocerus*, *Phyteumas*, and *Phymateus* are closely related, indicating their inclusion in the tribe Phymateini. The close relationships among Pyrgomorphid tribes and genera have previously been documented by several authors. For instance, Kevan et al. (1974) suggested a close relationship between Taphronotini and Dictyophorini according to copulatory structures. Similarly, Mariño-Perez and Song (2018) reported a close relationship between Taphronotini and Dictyophorini, as well as among *Zonocerus*, including *Zonocerus variegatus*, and *Phymateus*, including *Phymateus saxosus*.

When comparing our tree with the molecular phylogeny of Zahid et al. (2021), we found concordance regarding the monophyly of Dictyophorini. Similarly, we found concordance regarding the monophyly of Phymateini when comparing our phylogenetic tree with the morphological phylogenetic tree by Mariño-Pérez and Song (2018). In addition, the monophyly of Phymateini recovered in our tree was not supported by the molecular phylogeny of Zahid et al. (2021), as this tribe was found to be paraphyletic. In addition, Mariño-Pérez and Song (2019) reported that *Monistria* Stål, *Dictyophorus*, *Phymateus*, and *Poekilocerus* Serville were scattered throughout the phylogeny, forming paraphyletic groups. Such discordances in the topologies are not surprising, as previous studies, e.g., Baker et al. (1998), Friedrich et al. (2014), Kjer et al. (2016), and Peters et al. (2014), have demonstrated. However, as our study was limited in terms of taxon sampling to clarify the taxonomic position of *Parapetasia* and *Loveridgacris* species, we did not include many species from other tribes. Hence, we are not able to address these problems with our dataset.

We obtained robust evidence supporting the distinct status of the genus *Parapetasia*. Specifically, *Parapetasia rammei* has been confirmed as the sister taxon to *Parapetasia femorata*, and this distinction is further reinforced by morphological and phallic structure diagnostic traits. Furthermore, our phylogenetic tree revealed substantial genetic differentiation between the genera *Loveridgacris* and *Parapetasia*. Consequently, Kevan's (1977) proposal to synonymize *P. rammei* and *L. impotens* with *P. femorata*, primarily based on their shared geographic distribution and some morphological resemblances, is now questioned. This study marks the first integrative examination of the phylogeny of Dictyophorini, which revealed a consistently structured topology. Nonetheless, to fully resolve the phylogenetic relationships within Dictyophorini, it is imperative to include additional genera and their respective species in future investigations, as well as additional genetic markers.

The findings from the maximum likelihood (ML) and Bayesian inference (BI) analyses and the examination of the complete mitogenome indicate that it is challenging to establish a phylogenetic relationship between *L. impotens* and the newly described species *L. tectiferus* sp. nov. using the COI gene alone. Even the complete mitogenome revealed only minor divergence in this regard. Generally, it is likely that *L. tectiferus* sp. nov. represents a relatively young species in the early stages of speciation. To gain more conclusive insights into its taxonomic status and evolutionary trajectory, broader sampling of specimens is needed.

Conclusion

This study offers a reassessment of the Pyrgomorphid grasshopper genera *Parapetasia* and *Loveridgacris*, along with the first-ever analysis of the mitochondrial genome in the genus *Loveridgacris*. Our research unequivocally demonstrated that the genus *Parapetasia* comprises two distinct species, *P. femorata* and *P. rammei*, characterized by both pronounced morphological and genetic disparities. Additionally, we underscore the substantial differences, both morphologically and genetically, between the genera *Parapetasia* and *Loveridgacris*. Consequently, the previous doubts regarding their taxonomic position are dispelled. Therefore, we confirm that *Parapetasia* and *Loveridgacris* are unequivocally recognized as two distinct genera. Finally, we describe a new *Loveridgacris* species adding to the diversity of the group.

Acknowledgments

The authors are grateful to the Alexander von Humboldt Foundation for its financial support. The authors thank Cameroon's Ministry of Scientific Research and Innovation for granting the research permit for field collection (N 0000010/MINRESI/B00/C00/C10/C13). We also thank the Commission for Science and Technology, Tanzania and the Tanzania Wildlife Research Institute, Tanzania, for granting research permits. We thank the Mohamed bin Zayed Species Conservation Fund for their financial support. We would like to thank Dr. Ricardo Mariño-Pérez at the University of Michigan, Prof. Hojun Song at Texas A & M University, United States, and Mrs. and Katrin Elgner at the Senckenberg museum in Germany for providing us with the necessary literature. We are thankful to Mrs. Birgit Jaenicke at the Museum für Naturkunde Berlin for granting us permission to examine several samples. We thank Mr. Aristide Junior Sock Bell and Mr. Sedrick Junior Tsekane for their valuable assistance during field investigations in the Ebo Forest, Cameroon. The authors are grateful to Ms. Eileen Nguyen for her valuable support when taking the photographs. We would like to thank Mr. Carsten Bruns and Ms. Lara-Sophie Dey for their assistance in the laboratory. We also thank Mr. Jithin Johnson for the introduction to the mapping. Furthermore, we are grateful to the Academy of Natural Sciences of Philadelphia for providing photographs of the types *P. femorata* and *P. calabarica*. The authors are also grateful to the American Journal Experts (AJE) for editing the manuscript for proper English language.

References

Akbar SS, Kevan McEDK (1964) Two subgenera of Pyrgomorphidae (Orth., Acridoidea) raised to generic status on the basis of their phallic structures. Entomologist's Monthly Magazine 99: 90–95.

Baker RH, Yu X, DeSalle R (1998) Assessing the relative contribution of molecular and morphological characters in simultaneous analysis trees. Molecular Phylogenetics and Evolution 9(3): 427–436. https://doi.org/10.1006/mpev.1998.0519

Bolivar I (1904) Notas sobre los Pirgomorfidos (Pyrgomorphidae). Boletín de la Real Sociedad española de Historia natural 4: 89–111.

Bolivar I (1884) Monografia de los Pirgomorfinos. Anales de la Sociedad española de Historia natural 13: 419–500. [pls. 1–4]

Cigliano MM, Braun H, Eades DC, Otte D (2023) Orthoptera Species File. Version 5.0/5.0. http://Orthoptera.SpeciesFile.org [02.09.2023]

Dirsh VM (1956) The phallic complex in Acridoidea (Orthoptera) in relation to taxonomy. Transactions of the Royal Entomological Society of London 108(7): 223–356. https://doi.org/10.1111/j.1365-2311.1956.tb02270.x

Dirsh VM (1957) The spermatheca as a taxonomic character in Acridoidea (Orthoptera). Proceedings of the Royal Entomological Society of London. Series A, General Entomology 32(7–9): 107–114. https://doi.org/10.1111/j.1365-3032.1957.tb00380.x

Dirsh VM (1961) A preliminary revision of the families and subfamilies of Acridoidea (Orthoptera, Insecta). Bulletin of the British Museum (Natural History) Entomology 10: 351–419. https://doi.org/10.5962/bhl.part.16264

Dirsh VM (1965) The African genera of Acridoidea. Cambridge University Press for the Anti-Locust Research Centre, London, xiii + 579 pp.

Dirsh VM (1970) Acridoidea of the Congo (Orthoptera). Annales du Musée Royal de l'Afrique Centrale (série Sciences zoologiques), Tervuren 182: [6] + 605 pp.

Eades DC (2000) Evolutionary relationships of phallic structures of Acridomorpha (Orthoptera). Journal of Orthoptera Research 9(9): 181–210. https://doi.org/10.2307/3503648

Edgar RC (2004) MUSCLE: A multiple sequence alignment method with reduced time and space complexity. BMC Bioinformatics 5(1): 113. https://doi.org/10.1186/1471-2105-5-113

Folmer O, Black M, Hoeh W, Lutz R, Vrijenhoek R (1994) DNA primers for amplification of mitochondrial cytochrome *c* oxidase subunit I from diverse metazoan invertebrates. Molecular Marine Biology and Biotechnology 3: 294–299.

Friedrich F, Matsumura Y, Pohl H, Bai M, Hörnschemeyer T, Beutel RG (2014) Insect morphology in the age of phylogenomics: Innovative techniques and its future role in systematics. Entomological Science 17(1): 1–24. https://doi.org/10.1111/ens.12053

Grzywacz B, Warchałowska-Śliwa E, Kociński M, Heller K-G, Hemp C (2021) Diversification of the Balloon bushcrickets (Orthoptera, Hexacentrinae, *Aerotegmina*) in the East African mountains. Scientific Reports 11(1): 9878. https://doi.org/10.1038/s41598-021-89364-4

Hemp C, Kehl S, Schultz O, Wägele W, Hemp A (2015) Climatic fluctuations and topography as motor for speciation: case study on *Parepistaurus* Karsch, 1896 (Orthoptera: Acrididae, Coptacridinae). Systematic Entomology 40(1): 17–34. https://doi.org/10.1111/syen.12092

Hemp C, Heller K-G, Hemp A, Warchalowska-Sliwa E, Grzywacz B (2018) A molecular phylogeny of East African *Amytta* (Orthoptera: Tettigoniidae, Meconematinae) with data on their karyotypes. Systematic Entomology 43(2): 239–249. https://doi.org/10.1111/syen.12269

Hemp C, Scherer C, Brandl R, Pinkert S (2020) The origin of the endemic African grasshopper family Lentulidae (Orthoptera: Acridoidea) and its climate-induced diversification. Journal of Biogeography 47(8): 1805–1815. https://doi.org/10.1111/jbi.13880

Hochkirch A (1998) A comparison of the grasshopper fauna (Orthoptera: Acridoidea & Eumast acoidea) of the Uluguru mountains and the East Usambara mountains, Tanzania. Journal of East African Natural History 87(1): 221–232. https://doi.org/10.2982/0012-8317(1998)87[221:ACOTGF]2.0.CO;2

Johnston HB (1956) Annotated catalogue of African grasshoppers. Cambridge University Press for the Anti-Locust Research Centre, London, xxii + 883 pp.

Karsch F (1888) Beitrage zu Ignacio Bolivar's Monografia de los Pirgomorfinos (Madrid, 1884). Entomologisches Nachrichtenblatt (Vienna, Austria) 14(21): 328–335.

Kearse M, Moir R, Wilson A, Stones-Havas S, Cheung M, Sturrock S, Buxton S, Cooper A, Markowitz S, Duran C, Thierer T, Ashton B, Meintjes P, Drummond A (2012) Geneious Basic: An integrated and extendable desktop software platform for the organization and analysis of sequence data. Bioinformatics (Oxford, England) 28(12): 1647–1649. https://doi.org/10.1093/bioinformatics/bts199

Kevan DKM (1962) Pyrgomorphidae (Orthoptera: Acridoidea) collected in Africa by E.S. Ross and R.E. Leech, 1957–1958, with descriptions of new species. Proceedings of the California Academy of Sciences, fourth series 31(9): 227–248.

Kevan DKM (1977) Ordo Orthoptera s. str. (= Saltatoria-Caelifera) Subordo Acridodea Infraordo Acridomorpha Superfam. Acridoidea Fam. Pyrgomorphidae. In: Beier M (Ed.) Orthopterorum Catalogus, W. Junk, La Hague 16, iv + 656 pp. [+ 7 pp].

Kevan DKM, Akbar SS (1964) The Pyrgomorphidae (Orthoptera: Acridoidea): Their systematics, tribal divisions and distribution. Canadian Entomologist 96(12): 1505–1536. https://doi.org/10.4039/Ent961505-12

Kevan DKM, Akbar SS, Chang YC (1969) The concealed copulatory structures of Pyrgomorphidae (Orthoptera: Acridoidea). Part I. General introduction. Eos, Revista española de Entomología 44: 165–266.

Kevan DKM, Akbar SS, Chang YC (1972) The concealed copulatory structures of the Pyrgomorphidae (Orthoptera: Acridoidea). Part IV. Tribes Desmopterini, Monistriini, Chlorizeinini, Poekilocerini and Phymateini. Eos, Revista española de Entomología 47: 137–234.

Kevan DKM, Akbar SS, Chang YC (1974) The concealed copulatory structures of the Pyrgomorphidae (Orthoptera: Acridoidea). Part V. Tribes Schulthessiini, Taphronotini, Dictyophorini, Tagastini, Pseudomorphacridini, Atractomorphini, Sphenariini and Omurini. Eos, Revista española de Entomología 48: 203–294.

Kjer K, Borowiec ML, Frandsen PB, Ware J, Wiegmann BM (2016) Advances using molecular data in insect systematics. Current Opinion in Insect Science 18: 40–47. https://doi.org/10.1016/j.cois.2016.09.006

Mariño-Pérez R, Song H (2018) Phylogeny of the grasshopper family Pyrgomorphidae (Caelifera, Orthoptera) based on morphology. Systematic Entomology 43(1): 90–108. https://doi.org/10.1111/syen.12251

Mariño-Pérez R, Song H (2019) On the origin of the New World Pyrgomorphidae (Insecta: Orthoptera). Molecular Phylogenetics and Evolution 139: 106537. https://doi.org/10.1016/j.ympev.2019.106537

Martinelli AB, Waichert C, Barbosa DN, Fagundes V, Azevedo C (2017) The use of Proteinase K to access genitalia morphology, vouchering and DNA extraction in minute wasps. Anais da Academia Brasileira de Ciências 89(3): 1629–1633. https://doi.org/10.1590/0001-3765201720160825

Meng GL, Li YY, Yang CT, Liu S (2019) MitoZ: Atoolkit for animal mitochondrial genome assembly, annotation and visualization. Nucleic Acids Research 47(11): e63. https://doi.org/10.1093/nar/gkz173

Mestre J, Chiffaud J (2009) Acridiens du Cameroun et de République centrafricaine (Orthoptera Caelifera). Supplément au catalogue et atlas des acridiens d'Afrique de l'Ouest. http://acrida.info/PDF2009/Catalogue-Acridiens-2009.pd

Palumbi SR, Martin A, Romano S, McMillan WO, Stice L, Garbowski G (1991) The simple fools guide to PCR. A collection of PCR protocols, version 2. University of Hawaii, Honolulu.

Paxton RJ, Thorén PA, Tengö J, Estoup A, Pamilo P (1996) Mating structure and nestmate relatedness in a communal bee, *Andrena jacobi* (Hymenoptera, Andrenidae), using microsatellites. Molecular Ecology 5(4): 511–519. https://doi.org/10.1111/j.1365-294X.1996.tb00343.x

Perna NT, Kocher TD (1995) Patterns of nucleotide composition at fourfold degenerate sites of animal mitochondrial genomes. Journal of Molecular Evolution 41(3): 353–358. https://doi.org/10.1007/BF01215182

Peters RS, Meusemann K, Petersen M, Mayer C, Wilbrandt J, Ziesmann T, Donath A, Kjer KM, Aspöck U, Aspöck H, Aberer A, Stamatakis A, Friedrich F, Hünefeld F, Niehuis O, Beutel RG, Misof B (2014) The evolutionary history of holometabolous insects inferred from transcriptome-based phylogeny and comprehensive morphological data. BMC Evolutionary Biology 14(1): 52. https://doi.org/10.1186/1471-2148-14-52

Rambaut A (2010) FigTree v1.3.1. Institute of Evolutionary Biology, University of Edinburgh, Edinburgh. http://tree.bio.ed.ac.uk/software/figtree/

Rehn JAG (1953) Records and descriptions of Pyrgomorphinae (Orthoptera: Acrididae), with critical notes on certain genera. Transactions of the American Entomological Society 99: 99–149.

Rehn JAG (1954) Loveridgacris. Entomological News 65(5): 128.

Ronquist F, Teslenko M, Van Der Mark P, Ayres DL, Darling A, Hohn S, Larget B, Liu L, Suchard MA, Huelsenbeck JP (2012) MrBayes 3.2: Efficient Bayesian Phylogenetic Inference and Model Choice Across a Large Model Space. Systematic Biology 61(3): 539–542. https://doi.org/10.1093/sysbio/sys029

Rowell CHF (2013) The grasshoppers (Caelifera) of Costa Rica and Panama. The Orthopterists' Society, 611 pp.

Rowell CHF, Hemp C, Harvey AW (2015) Jago's Grasshoppers of East and North East Africa, Vol. 1: Pneumoridae, Pyrgomorphidae, Lentulidae, Pamphagidae, and Dericorythidae. San Francisco, Blurb Publishers, 237 pp.

Seino RA, Njoya MTM (2018) Species diversity of pyrgomorphidae (Orthoptera: Caelifera) grasshoppers in the North West region of Cameroon. International Journal of Zoology and Applied Biosciences 3(1): 104–109.

Song H, Amédégnato C, Cigliano MM, Desutter-Grandcolas L, Heads SW, Huang Y, Otte D, Whiting MF (2015) 300 million years of diversification: Elucidating the patterns of orthopteran evolution based on comprehensive taxon and gene sampling. Cladistics 31(6): 621–626. https://doi.org/10.1111/cla.12116

Tamura K, Stecher G, Kumar S (2021) MEGA11: Molecular Evolutionary Genetics Analysis Version 11. Molecular Biology and Evolution 38(7): 3022–3027. https://doi.org/10.1093/molbev/msab120

Zahid S, Mariño-Pérez R, Song H (2021) Molecular phylogeny of the grasshopper family Pyrgomorphidae (Caelifera, Orthoptera) reveals rampant paraphyly and convergence of traditionally used taxonomic characters. Zootaxa 4969(1): 101–118. https://doi.org/10.11646/zootaxa.4969.1.5

Supplementary material 1

Complete mitochondrial genomes of *Loveridgacris impotens* and *Loveridgacris tectiferus* sp. nov.

Authors: Jeanne Agrippine Yetchom Fondjo, Martin Husemann, Armand Richard Nzoko Fiemapong, Alain Didier Missoup, Martin Kenne, Maurice Tindo, Oliver Hawlitschek, Tarekegn Fite Duressa, Sheng-Quan Xu, Wenhui Zhu, Claudia Hemp

Data type: tif

Explanation note: In this supplementary material, the mitogenomes of *Loveridgacris impotens* and *Loveridgacris tectiferus* sp. nov. are presented. The lenght of the genomes, their organization and nucleotide composition are also shown on the file.

Link: https://doi.org/10.3897/dez.71.125877.suppl1

Supplementary material 2

Genetic distance of the 13 protein-coding genes between *Loveridgacris impotens* and *Loveridgacris tectiferus* sp. nov.

Authors: Jeanne Agrippine Yetchom Fondjo, Martin Husemann, Armand Richard Nzoko Fiemapong, Alain Didier Missoup, Martin Kenne, Maurice Tindo, Oliver Hawlitschek, Tarekegn Fite Duressa, Sheng-Quan Xu, Wenhui Zhu, Claudia Hemp

Data type: tif

Explanation note: This supplemtary material shows the pairwise genetic distances inferred from all 13 protein-coding genes between *Loveridgacris impotens* and *Loveridgacris tectiferus* sp. nov.

Link: https://doi.org/10.3897/dez.71.125877.suppl2

Supplementary material 3

Localities and coordinates of *Parapetasia* and *Loveridgacris*

Authors: Jeanne Agrippine Yetchom Fondjo, Martin Husemann, Armand Richard Nzoko Fiemapong, Alain Didier Missoup, Martin Kenne, Maurice Tindo, Oliver Hawlitschek, Tarekegn Fite Duressa, Sheng-Quan Xu, Wenhui Zhu, Claudia Hemp

Data type: docx

Link: https://doi.org/10.3897/dez.71.125877.suppl3